Research Square

Preprints are preliminary reports that have not undergone peer review.
They should not be considered conclusive, used to inform clinical practice,
or referenced by the media as validated information.

A single versus multi-vector approach to treating post-traumatic osteoarthritis using scAAV2 IL-1ra or scAAV2 IL-1ra/IGF-I in an equine preclinical model

Jaiden H. Oropallo
Colorado State University
Parvathy Thampi
Colorado State University
Jennifer N. Phillips
Colorado State University
Myra F. Barrett
Colorado State University
Katie A. Seabaugh
Colorado State University
Lyndah Chow
Colorado State University
Ann M. Hess
Colorado State University
Lynn M. Pezzanite
Colorado State University
Lester Suárez-Amarán
Colorado State University
Constance R. Chu
Stanford University
C. Wayne McIlwraith
Colorado State University
Richard Jude Samulski
University of North Carolina at Chapel Hill
Brad B. Nelson
Colorado State University
Laurie R. Goodrich
Laurie.Goodrich@colostate.edu

Colorado State University

Research Article

Keywords:

Posted Date: March 8th, 2026

DOI: https://doi.org/10.21203/rs.3.rs-8960268/v1

License: This work is licensed under a Creative Commons Attribution 4.0 International License.
Read Full License

Additional Declarations: No competing interests reported.

Abstract

Interest in leveraging FDA approved "self-complementary" adeno-associated viral (scAAV) vectors for osteoarthritis treatment has been steadily rising. Due to the multi-faceted nature of osteoarthritis (an inflammatory/catabolic environment), we investigated the efficacy of a combined scAAV-based gene therapy approach to treating post-traumatic osteoarthritis (PTOA) in an equine preclinical model. Two approaches were established using scAAV2IL-1ra either alone or in combination with scAAV2IGF-I. All therapeutic proteins increased in the joints over the 4-month study period, (IL-1ra 218-300x & IGF-I 4x). Primary outcome measures, including clinical exams, MRI scoring, and gross and histological scoring of the joints revealed that scAAV2IL-1ra treatment alone consistently demonstrated the least PTOA progression. Surprisingly, the combination treated group (scAAV2IL-1ra + scAAV2IGF-I) demonstrated greater PTOA progression than the untreated controls. Exploratory data suggest this unexpected outcome may not be due to therapeutic transgenes but to dose-related, vector-induced immune responses. In summary, our observations strongly support optimizing scAAV for joint transduction & utilizing the highly translational equine model at reduced viral doses.

Introduction

Osteoarthritis (OA) is a prevalent degenerative joint disease estimated to affect over 14% of the adult population in the United States (around 35–40 million people) [1]. It is characterized by the breakdown of articular cartilage and joint tissues, leading to pain and impaired mobility. Aside from its debilitating physical effects, OA also creates a massive healthcare and economic burden. It is the 15th highest cause of years lived with disability, and was the second most costly medical condition treated in US hospitals in 2013 (18.4 billion total) [2, 3]. While OA is most commonly associated with aging, it can also result from significant joint injuries in younger individuals, leading to post-traumatic osteoarthritis (PTOA). PTOA is especially prevalent in the military, identified as the primary source of disability in warfighters [4]. It has been shown that approximately 60% of battlefield injuries to joints will result in PTOA progression and degradation of articular cartilage. Further, if the knee is specifically affected, the probability of progression to degenerative joint disease is close to 100% [4]. Finally, OA and PTOA are also significant issues in equine athletes, with OA-induced cartilage degradation in metacarpophalangeal joints ending the careers of one-third of 2- and 3-year old racehorses [5]. In addition, PTOA-induced lameness in racehorses is identified as the primary factor contributing to diminished athletic function and loss of performance [6–9].

Current drug therapies to treat PTOA for both humans and horses usually result in mild to moderate symptom relief and do relatively little to modify disease progression caused by inflammation and matrix degradation [10, 11]. Significant disease modification strategies have remained elusive; treatment in most cases is palliative and continues to result in significant side effects such as gastropathy, nephropathy and cardiac disease [12]. Over the past 15 years, many promising regenerative therapies have emerged, providing valuable proof of concept and foundational knowledge for OA/PTOA treatments. In particular, recombinant Adeno-Associated Viral (rAAV) vectors have demonstrated

substantial therapeutic benefit across a wide range of diseases. Supported by a strong safety profile and well-established clinical efficacy, rAAV-based gene therapy has led to the regulatory approval of nine products—Glybera, Luxturna, Zolgensma/Itvisma, Upstaza/Kebilidi, Elevidys, Roctavian, Hemgenix, BEQVEZ, and BBM-H901—by major regulatory agencies, including the U.S. Food and Drug Administration, the European Medicines Agency, and China's National Medical Products Administration [13–21]. In the field of OA/PTOA, rAAV vectors have shown considerable promise in achieving sustained, long-term expression of therapeutic proteins within the joint and are currently being evaluated in multiple Phase I clinical trials in humans for the treatment of joint-related diseases, including OA [22–28]. However, the long-term benefits of these therapies for OA/PTOA treatment have so far failed to reverse the progressive breakdown of joint tissues or prevent reinjury. OA results from an imbalance between anabolic and catabolic factors, with pro-inflammatory cytokines and catabolic processes outweighing anti-inflammatory cytokines and anabolic pathways [29]. Many current treatment strategies typically focus on a single gene, targeting either inflammation or anabolic processes rather than addressing the disease's multifaceted nature [30]. To establish long-term healing in the joint we investigated the efficacy of a gene therapy approach utilizing equine interleukin-1 receptor antagonist (IL-1ra) to modulate inflammation in the joint combined with equine insulin-like growth factor-1 (IGF-I) to stimulate cartilage healing.

Inflammation in the joint has long been recognized as a major driver of OA and PTOA [31–34]. Among these inflammatory processes, interleukin-1beta (IL-1β) is known to upregulate a number of inflammatory cytokines and catabolic enzymes, including tumor necrosis factor alpha, interleukin-6, nitric oxide, matrix metalloproteinases − 1, -3, -9, and − 13, as well as a disintegrin and metalloproteinase with thrombospondin motifs − 4 and − 5 [35–41]. As such, interruption of IL-1β signaling represents a potent target by which to modulate inflammation in the joint. To downregulate IL-1β signaling, many studies have investigated the efficacy of its natural antagonist, IL-1ra [42–48]. A major shortcoming of direct IL-1ra intra-articular injection is that IL-1ra has a short half-life (days) and, although an initial therapeutic effect results following injection, long-term relief of pain, restoration of mobility, and the desired effect of disease modification have remained elusive until extended intra-articular production can be achieved [49, 50]. Utilizing gene therapy to extend the production of IL-1ra within the joint is a logical and realistic approach to fulfill the need for long-term intra-articular production of IL-1ra. In fact, gene therapy preclinical trials using IL-1ra in rats, mice, and rabbits have revealed significant increases in IL-1ra production using adenoviral, retroviral and lentiviral vectors, leading to suppression of inflammation in PTOA affected joints [51–53]. When IL-1ra gene therapy using an adenoviral vector was administered intra-articularly in the osteochondral chip fragment model of equine PTOA, a significant reduction of pain and preservation of articular cartilage resulted [54]. Further, when IL-1ra was delivered ex vivo to joints of patients with severe inflammation associated with rheumatoid arthritis in two separate studies, patients had significantly elevated levels of IL-1ra intra-articularly with significant pain reduction [55, 56]. To leverage IL-1ra's anti-inflammatory properties, our group previously engineered a self-complementary AAV2 (scAAV2) equine codon-optimized IL-1ra (scAAV2IL-1ra) vector designed to increase IL-1ra expression in equine joints with minimal vector-induced immune reaction [43].

While IL-1ra-induced expression via a gene therapy approach holds promise in attenuating OA-induced inflammation, direct healing and regeneration of damaged articular cartilage remains elusive. To support complete and sustained joint healing through promotion of tissue regeneration the activation of anabolic signaling may be essential. To that end, the authors of this study delivered two separate scAAV2 vectors to upregulate expression of both IL-1ra and IGF-I. IGF-I is a potent anabolic promoter of cartilage repair that acts through up-regulation of chondrocyte proliferation, extracellular matrix production and collagen type II content [57, 58]. Previous studies utilizing IGF-I delivered through gene therapeutic mechanisms have shown robustly enhanced repair mechanisms of articular cartilage [59–63]. Our group has shown that delivery of IGF-I through gene therapeutic mechanisms using an adenoviral vector significantly up-regulated IGF-I, although protein production was short-lived (21 days) [64]. However, despite short-term up-regulation of protein using an adenoviral vector, significant enhancement of early chondral healing resulted with this therapy [65]. Other groups have reported similar healing patterns utilizing rAAV-mediated delivery of IGF-I to treat OA in large animal models, including increased collagen type II content [66, 67], subchondral bone repair [66], minimal immune response [68], and improved cartilage defect healing [66, 67, 69]. Considering these studies in combination with our own previous work with IGF-I, we hypothesized that achievement of long-term IGF-I protein production in joints through *in vivo* delivery of a scAAV2IGF-I vector in combination with scAAV2IL-1ra would likely result in improved cartilage healing compared to a scAAV2IL-1ra vector alone. To accomplish this, our group previously engineered an equine codon optimized scAAV2IGF-I vector that generates high levels of IGF-I *in vitro* and has been demonstrated to up-regulate collagen and GAG production in equine chondrocytes [70].

The use of rAAV to express multiple therapeutic proteins simultaneously to treat OA has been investigated by several groups. *In vitro* studies have demonstrated the ability of rAAV to induce expression of multiple therapeutic proteins simultaneously, leading to increased cell proliferation and extra-cellular matrix production in both chondrocytes and human mesenchymal stem cells [71, 72]. A study combining rAAV-induced expression of IL-1ra as an anti-inflammatory with an anabolic factor (in this case sex-determining region Y-type high mobility group box 9 or SOX9) to treat OA was recently reported [73]. The combined IL-1ra/SOX9 treatment (two separate vectors administered simultaneously) was able to more effectively inhibit pro-inflammatory signaling and maintain cartilage homeostasis as compared to rAAV-IL-1ra or rAAV-SOX9 treatments alone in a surgically induced rat OA model, demonstrating the potential of combination rAAV treatments for OA *in vivo*. Co-expression of IL-1ra and IGF-I has been previously investigated by our group, providing an important proof-of-concept that combined IL-1ra/IGF-I gene therapeutics have the potential to address multiple facets of OA simultaneously [74]. However, this study also showed that adenoviral delivery of IL-1ra and IGF-I may not be sufficient to induce therapeutically relevant levels of IGF-I protein in the joint. To address this, we employed a recombinant scAAV vector, which circumvents the rate-limiting second-strand DNA synthesis step inherent to single-stranded AAV (ssAAV) vector transduction. This feature allows scAAV vectors to achieve faster and more efficient transgene expression during cellular transduction, resulting in significantly greater transduction efficiency and more sustained therapeutic protein expression compared with ssAAV vectors [59, 60]. While scAAV offers higher efficiency than ssAAV, both delivery

methods are still susceptible to the presence of neutralizing antibodies (NAbs). Pre-existing NAbs to AAV2 are common in humans, often exceeding 50% and sometimes reaching over 80–90% in adults, with significant variation by age, geography, and gender [75–78]. Similarly, presence of NAbs to AAV2 has been found in a number of animal species commonly used as translational models of OA research, including mice, rabbits, sheep and dogs [79, 80]. While some animal models have shown that pre-existing AAV-specific NAbs may have negligible effects on rAAV infectivity, further elucidation of the impact of AAV-specific NAbs, as well as NAb generation following vector administration that may preclude vector re-dosing, is crucial for determining both optimal vector dosing and the feasibility of re-dosing strategies [67].

Due to the inability of currently designed gene therapeutic treatments to fully address multiple facets of OA simultaneously, we proposed a novel scAAV2-mediated approach to deliver a combination of an anti-inflammatory cytokine (IL-1ra) and a pro-anabolic growth factor (IGF-I) in a well-validated experimental joint model of equine PTOA by delivering two vectors simultaneously. Our objective was to examine if administration of scAAV2IL-1ra and scAAV2IGF-I (either scAAV2IL-1ra alone or in combination with scAAV2IGF-I) in this model would lead to improved functional outcomes, with the long-term goal of further testing in Phase I preclinical studies in horses. We hypothesized that administration of a combination of scAAV2IL-1ra and scAAV2IGF-I in an equine model of PTOA would result in superior clinical outcomes and enhanced joint healing compared to joints treated with scAAV2IL-1ra alone, as evidenced by improved clinical, macroscopic, histological and imaging scoring of PTOA joints.

Materials & Methods

Experimental design overview

Twenty-five skeletally-mature horses aged 2–5 years with no radiographic abnormalities within the carpus nor signs of lameness were approved by the Institutional Animal Care and Use Committee (protocol #1517) for use in this study. All horses had an osteochondral chip fragment surgically created in one randomly selected middle carpal joint to produce experimental PTOA, while the opposite joint served as the sham control. Fourteen days after surgery, treated horses were injected intra-articularly with scAAV2IL-1ra alone or combined scAAV2IL-1ra and scAAV2IGF-I (dose established in our pilot *in vivo* dose titration study – 5×10^{11} vg scAAV2 EqIL-1ra [44]) diluted to a total volume of 5 mL with phosphate buffered saline (PBS) in the joint with the osteochondral chip fragment, while the opposite non-fragmented (normal) joint received an equal volume of PBS. Each of the two scAAV treatment groups had 8 horses per group, while a third control group of 7 horses (the ‘untreated’/saline control group) received an intra-articular injection of 5 mL PBS in both the fragmented (PTOA) and non-fragmented (normal) middle carpal joints (Fig. 1A).

Induction of osteoarthritis

The osteochondral chip fragments were created using arthroscopic guidance by an American College of Veterinary Surgeons board-certified surgeon as previously described [42, 54]. Briefly, an 8 mm osteochondral fragment was created in one randomly chosen middle carpal joint of each horse. Exposed subchondral bone between fragment and parent bone was debrided using a motorized arthroburr to form a 15 mm wide defect bed (Fig. 1B). Diagnostic arthroscopy was also performed on the contralateral middle carpal joint (sham) to confirm the absence of any significant intra-articular lesions.

Exercise protocol and clinical examinations

Exercise on a high-speed treadmill began for all horses 14 days after fragment creation and continued 5 days per week until Day 112 (four months post-surgery) as previously described, simulating athletic conditions commonly seen in horses developing osteochondral fragmentation and subsequent OA [8, 42]. Clinical outcomes were recorded on Day 0 (surgery date) and every two weeks following through the study period. This included exams conducted by an American College of Veterinary Sports Medicine and Rehabilitation board-certified veterinarian blinded to treatment assignment for subjective lameness, flexion, synovial effusion, and range of motion in each forelimb, followed by an objective lameness exam using the Lameness Locator (Equinosis, Columbia, MO, USA) as previously described [81, 82].

Imaging outcomes

Bilateral carpal radiographic examinations (anterior–posterior and flexed lateral) were performed before PTOA induction, at treatment administration (Day 14), and then every 50 days following PTOA induction. Radiographs were graded by an American College of Veterinary Radiologists (ACVR) board-certified radiologist blinded to treatment assignment using a 0–4 grading scale (none, very mild, mild, moderate and severe) for assessment of changes in the subchondral bone (lysis and sclerosis), for joint capsule enthesopathy, and for peri-articular osteophyte formation (PAOF). The 0–4 scores for each of the four aforementioned parameters were then summed to give a total 0–16 score for each joint. An MRI was performed at the endpoint of the study on each limb and graded by an ACVR board-certified radiologist blinded to treatment assignment on a 0–4 (normal, slight change, mild change, moderate change, severe change) scale for synovial effusion, synovial proliferation, joint capsule thickness, joint capsule edema, bone edema and sclerosis of the radial carpal and third carpal bones. The 0–4 scores for each of the seven aforementioned parameters was then summed to give a total 0–28 score for each joint.

Synovial fluid analysis

Synovial fluid (~ 2 mL) was collected at the time of surgery and then every 2 weeks until termination of the study at Day 112. The samples were immediately centrifuged at 1200xg and aliquots of the supernatant were stored at -80°C. Analysis of synovial fluid IL-1ra (ELISA, R&D Systems, Minneapolis, MN, USA), IGF-I (ELISA, R&D Systems), Prostaglandin E_2 (PGE_2) (ELISA, Enzo Life Sciences, Farmingdale, NY, USA), Interleukin-1 Beta (IL-1β) (Luminex MILLIPLEX Multiplex, Millipore Sigma, St. Louis, MO, USA), and Tumor Necrosis Factor Alpha (TNFα) (Luminex MILLIPLEX Multiplex) concentrations were performed according to manufacturer protocols. Concentrations below the standard curve were reported

as the lower limit of detection for each assay, an assay-specific value listed in the subtitles of Figs. 2 & 3 for each analyte tested.

Serum Neutralizing Antibody Titers: Whole blood samples were aspirated from each horse at Days 14 (pretreatment), 56 and 98. Samples were immediately centrifuged at 1200g for 10 min and serum aliquots were subsequently stored at -80°C. To determine NAb titer, HEK-293 cells were plated at 30000 cells/well in 96 well plates and allowed to equilibrate overnight. Serum samples were mixed with plain media at neat, 1:2, 1:5, 1:50, 1:500, 1:5000, and 1:10000 serum dilutions to a total volume of 50uL. Serum dilutions were then mixed with 50uL of 4000 vg/cell scAAV2 expressing green fluorescent protein (GFP) (Azenta, Burlington, MA, USA) diluted in plain media and the 100uL complexes were incubated at 37°C for 1 hour. After 1 hour media in the 96 well plates were aspirated and the serum/vector complexes were added to the cells. Serum/vector complexes were allowed to incubate with the cells for 3 hours, after which media was changed. Twenty-four hours after complexes were removed, the cells were lifted from the well plates and resuspended in eBioscience Flow Cytometry Buffer (ThermoFisher, Waltham, MA, USA). Flow cytometry was performed to determine the percent of cells expressing GFP with the Attune NxT (ThermoFisher). Neutralizing antibody titers per sample were defined as the lowest dilution in which percent GFP expression was equal to or greater than 50% of the positive control (50uL of 4000 vg/cell mixed with 50uL neat media) [45, 83, 84].

Postmortem examination

The horses were euthanized at Day 112 and each middle carpal joint was aseptically prepared for gross examination. Middle carpal joints were disarticulated and subjectively scored by two ACVS board-certified veterinarians blinded to treatment assignments for features of cartilage erosion and synovial inflammation. The severity (0–3) and extent (0–4) of cartilage erosions were scored for each individual carpal bone (radial, 2nd, 3rd, 4th, intermediate and ulnar bones), with a total score derived from the sum of the severity times erosion scores for each carpal bone as previously described [85]. Synovial inflammation was graded by summing synovial hyperemia (0–3) and hyperplasia (0–3) in the joint [85].

Histological evaluation of articular cartilage and synovial membrane

All samples taken for histological evaluation were placed in 10% buffered formalin immediately after collection, stained with hematoxylin and eosin, and graded by two ACVS board-certified veterinarians blinded to treatment assignments. Synovial membrane was harvested from medial, middle, and lateral aspects of the middle carpal joint. Five-micron sections were graded for cellular infiltration, synovial intimal hyperplasia, subintimal edema, subintimal fibrosis and vascularity on a 0–4 scale as previously described [81, 86]. Total scores for each synovial aspect were determined by summing the 0–4 score for each of the five aforementioned parameters (0–20 possible), with a final summed score determined by summed the total score across all three synovial aspects per joint (0–60 possible). Five mm^2 articular cartilage pieces were obtained from the radial, 2nd, 3rd, 4th, and ulnar carpal bones in each joint (see Fig. 1B). Articular cartilage sections were then evaluated for cartilage fibrillation, chondrocyte necrosis, chondrone formation (chondrocyte division within a lacuna) and focal loss of cells. Scores ranging from

0–4 were assigned to each measured parameter, as previously described [86]. Total scores for each carpal bone were determined by summing the 0–4 score for each of the four aforementioned parameters (0–16 possible), with a final summed score determined by summing the total score across all five carpal bones scored per joint (0–80 possible).

Statistical analysis

Statistical analysis was completed using R (version 2024.09.1 + 394) [87]. Power analysis for this experimental design was performed using outcome parameters of articular cartilage erosion and synovial cellular hyperplasia. Utilizing an effect size of 0.9 and standard deviation of 0.5, a power of 0.922 could be achieved with an N of 8 animals per group (one animal was removed from the saline treated group due to post-surgery colic, giving N = 7). Statistical analysis for conducted for five clinical variables (lameness, flexion, effusion, range of motion, and objective lameness), three synovial fluid biomarkers (IL-1ra, IGF-I, and PGE_2), two imaging outcomes (radiographic OA total score and MRI OA total score), two gross examination scores (cartilage erosion total score and synovial inflammation total score), six cartilage histological scoring totals (2nd carpal, 3rd carpal, 4th carpal, radial carpal, ulnar carpal and total score summed across carpals) and four synovium histological scoring totals (medial, center, and lateral synovium aspects as well as total score summed across aspects).

A linear mixed effects model was fit separately for most response variables. Fixed effects include treatment/OA status of each joint (joints classified as either sham/no treatment, OA/saline treatment, OA/IL-1ra treatment, or OA/combined IL1-ra and IGF-I treatment), and day of collection (if applicable) plus interaction. Random effects included subject and subject*OA when applicable (to capture effects of the joint over repeated measures). F-tests for main effects and interaction were considered. If there was statistical evidence of a treatment/OA effect or treatment*day interaction, then Tukey adjusted pairwise comparisons were used to compare between treatments separately at each time point. An estimated marginal means test with a Tukey adjustment was used to estimate and test comparisons of interest in line with analyses conducted in similar studies [88]. Residual diagnostic plots were used to check assumptions (normality and equal variance). Non-parametric methods were used for outcomes that did not satisfy assumptions (synovial fluid IL-1ra and IGF-I concentrations and improvement in lameness scores). Specifically, a Kruskal-Wallis test was used, followed by Dunn's post-hoc test for specific comparisons if there was statistical evidence of interaction. Significance for all tests were established at $P \leq 0.05$.

To estimate the clinical relevance of outcome measures Cohen's d was used to calculate effect size between groups when appropriate. Cohen's d was calculated between the saline control group and both the scAAV2IL-1ra and scAAV2IL-1ra/scAAV2IGF-I treated groups for improvement in lameness, MRI total score, cartilage erosion total score, cartilage histology total summed score, synovial inflammation total score, and synovium histology total summed score. An effect size of 0.2 was considered small, 0.5 medium, and 0.8 large.

(A) Schematic of treatment and control groups, defined by the presence or absence of an osteochondral chip fragment (PTOA induction) in the equine middle carpal joint, with intra-articular administration of scAAV2IL-1ra, combined scAAV2IL-1ra/scAAV2IGF-I, or saline treatment 14 days following surgery. **(B)** An illustration of the equine middle carpal joint indicating the area where the osteochondral chip fragment was induced (close-up view shown to the left). The empty black boxes indicate areas of the carpal bones where articular cartilage samples were taken for histology (CR-radial carpal, CU-ulnar carpal, C2-second carpal, C3-third carpal, and C4-fourth carpal). Diagram adapted from Goodrich et al, *Journal of the American Veterinary Medical Association*, 2024 with permission. **(C)** Study timeline indicating treatment administration, clinical data, and sample collection. Dots above the timeline indicate points for lameness exams, synovial fluid aspiration, blood collection, radiographs, and MRI.

Results

In this study, PTOA was induced in one middle carpal joint of each horse, with the contralateral joint serving as the sham operated, non-PTOA control. Horses were divided into 3 treatment groups, with each horse receiving an scAAV2 treatment or saline control intra-articularly in the PTOA-induced joint and a saline control intra-articularly in the sham operated control. Induction of PTOA in this model was validated by multiple outcome measures over the study period, most notably through clinical outcomes and radiographic scoring of OA features in the joints.

Synovial Fluid Evaluation

Mean IL-1ra levels in the synovial fluid revealed a statistically significant increase at all time points following treatment injection on Day 14 in both the scAAV2IL-1ra treated group and scAAV2IL-1ra/scAAV2IGF-I treated group as compared to the control groups (Fig. 2A; p-values listed in Appendix A). Mean synovial fluid IL-1ra levels peaked in the scAAV2IL-1ra/scAAV2IGF-I treated joints at Day 28, while mean levels peaked in the scAAV2IL-1ra treated joints at Day 42. These peaks respectively reflected an average 218x fold and 300x fold increase in mean IL-1ra concentration as compared to joints that did not receive the scAAV2IL-1ra vector. The mean IL-1ra levels in joints of both groups treated with the scAAV2IL-1ra vector remained elevated through the end of the study period (Day 112), demonstrating a 19x fold increase in mean IL-1ra levels in the scAAV2IL-1ra/scAAV2IGF-I treated joints and a 23x fold increase in mean IL-1ra levels in the joints of scAAV2IL-ra treated group as compared to joints that did not receive the scAAV2IL-1ra vector. Mean IL-1ra levels in the joints of horses in groups that did not receive the scAAV2IL-1ra vector (saline control group and non-OA sham control group) were almost entirely below the assay limit of detection (0.31 ng/mL) throughout the study period.

Mean IGF-I levels in the synovial fluid were marginally elevated at all time points following treatment injection on Day 14 in the scAAV2IL-1ra/scAAV2IGF-I treated group (Fig. 2B). Mean synovial fluid IGF-I levels peaked in the scAAV2IL-1ra/scAAV2IGF-I treated joints on Day 70, a 4.5x fold increase in mean IGF-I levels as compared to the joints that did not receive the scAAV2IGF-I vector (the scAAV2IL-1ra

treated group, saline control group, and non-OA sham control group). The scAAV2IL-1ra/scAAV2IGF-I treated joints showed a statistically significant increase in mean IGF-I levels as compared to all joints that did not receive the scAAV2IGF-I vector at a majority of time points following treatment administration (p-values listed in Appendix A), and demonstrated statistically significant increases compared to at least two of the three groups that did not receive the scAAV2IGF-I treatment at every time point following Day 14 (treatment injection). Mean IGF-I levels in the joints that did not receive the scAAV2IGF-I vector were mostly below the assay lower limit of detection (81.25 pg/mL) at all time points, with IGF-I levels in some joints slightly above the assay's lower limit of detection predominantly in Days 56 through 84.

An elevation in synovial fluid PGE_2 levels was observed in all groups from Day 0 to Day 14 (Fig. 3). Mean PGE_2 levels continued to increase in all groups at Day 28, with the exception of the scAAV2IL-1ra treated group, which showed similar mean PGE_2 levels between Day 14 and Day 28. Notably, mean PGE_2 levels in the scAAV2IL-1ra treated group significantly decreased at Day 42 as compared to the saline control group (p-value = 0.0103). This coincided with the highest mean IL-1ra levels reported over the study period for either group treated with the scAAV2IL-1ra vector (92.3 ng/mL, a 300x fold increase in mean IL-1ra levels as compared to the groups that did not receive the scAAV2IL-1ra vector). Mean PGE_2 levels were similar across groups for the remainder of the study. In addition to PGE_2, concentrations of the inflammatory markers IL-1β and TNFα in the synovial fluid were analyzed. Levels of both biomarkers were below the lower limit of detection of the multiplex assay (29 pg/mL for IL-1β and 4 pg/mL for TNFα) over the study period (data not shown).

Serum Neutralizing Antibody Effect

To determine the potential effect of vector dose ($5x10^{11}$ vg for scAAV2IL-1ra treated and $1x10^{12}$ vg for scAAV2IL-1ra/scAAV2IGF-I treated) on AAV2 neutralizing antibody formation over the study period, serum AAV2 NAb titers were determined for each horse before treatment administration (Day 14), at Day 56, and at Day 98. Almost all NAb titers were low (neat or 1:2) in both treatment and control groups before treatment administration, with the exception of two horses in the scAAV2IL-1ra/scAAV2IGF-I treated group, which demonstrated much higher levels of AAV2 NAbs (1:50 and 1:500 titers respectively, Fig. 4A). In regard to NAb formation, titers in the saline control group remained relatively low through Day 98. In contrast, both the scAAV2IL-1ra treated and scAAV2IL-1ra/scAAV2IGF-I treated group had overall higher titers at Day 56 as compared Day 14, indicating that scAAV2 administration promoted increased AAV2 NAb formation in the serum (Fig. 4B). On average titers were lower in the scAAV2IL-1ra treated group as compared to the scAAV2IL-1ra/scAAV2IGF-I treated group at Day 56, indicating that the increased viral dose in the scAAV2IL-1ra/scAAV2IGF-I treated group promoted increased AAV2 NAb formation. This is supported by the further increase in titer in most horses in the scAAV2IL-1ra/scAAV2IGF-I treated group at Day 98, while titers in the scAAV2IL-1ra treated group stayed the same or decreased (Fig. 4C). Titers for each individual horse over time are provided in Supplemental Material.

Clinical Outcomes

Mean lameness grades rose in all three PTOA-induced limb groups from Day 0 (PTOA induction) to Day 14, indicating successful induction of clinical features of PTOA (see Supplemental Figures). Mean lameness grades were similar between treated groups over the duration of the study period, with high variability within groups. Objective lameness scores (using the Equinosis lameness locator) were similar to the subjective lameness scores, with no statistically significant differences detected between groups at any time points (data not shown).

Mean improvement in lameness (calculated as the Day 14 lameness grade minus the Day 112 lameness grade) was highest in the scAAV2IL-1ra treated group, which showed an improvement in lameness score roughly 0.2 grades greater than the saline control group (0.75 grade average improvement vs 0.57, Fig. 5). The saline control group showed the second highest mean improvement in lameness score, followed by the scAAV2IL-1ra/scAAV2IGF-I treated group. The non-OA sham group showed a negative mean improvement in lameness score, suggesting a progressive increase in lameness from Day 14 to Day 112. Both the scAAV2IL-1ra treated and saline control group showed statistically significant increases in improvement in lameness compared to the non-OA sham control (p-values = 0.009 & 0.0266 respectively), with scAAV2IL-1ra demonstrating the greatest improvement. To estimate the clinical relevance of the scAAV2 treatments relative to the saline control Cohen's d was calculated as a measure of the magnitude of difference between groups (effect size). The scAAV2IL-1ra treated group had an effect size of 0.19, indicating a *relatively small positive effect* (greater improvement in lameness) compared with the saline control, while the scAAV2IL-1ra/scAAV2IGF-I treated group had an effect size of − 0.23, indicating a *small negative effect* (less improvement in lameness).

Flexion scores increased in all three PTOA-induced groups from Day 0 to Day 14, after which scores between groups were similar through the remainder of the study period. Similar to improvement in lameness, the improvement in flexion score from Day 14 to Day 112 was highest (greatest improvement) in the scAAV2IL-1ra treated group, although differences in flexion improvement between treated groups were also not statistically significant. Synovial effusion scores also rose in all PTOA-induced groups from Day 0 to Day 14, then remained similar over the remainder of the study period. Finally, range of motion scores rose slightly in PTOA-induced groups between Day 0 and Day 14, then attenuated to near 0 (normal) for the remainder of the study period (data for flexion, synovial effusion, and range of motion not shown).

Imaging Outcomes

Mean radiographic OA total scores in all three PTOA-induced groups demonstrated statistically significant increases as compared to the non-OA sham group at all time points after surgery, indicating that PTOA progression was successfully induced (see Supplemental Figures). Mean bone lysis, bone sclerosis, and joint capsule enthesopathy scores were similar between all treated groups (data for individual radiographic scoring metrics not shown). Mean peri-articular osteophyte formation score had

the largest differences between treated groups, with the scAAV2IL-1ra treated group receiving the lowest average PAOF scores (least osteophyte formation) of the PTOA induced groups at Days 56 and 112. Representative radiographs highlighting peri-articular osteophyte formation are shown in Fig. 7A.

Mean MRI OA total score showed a statistically significant increase (greater OA progression) in all of the PTOA-induced limb groups as opposed to the non-OA sham control group at the endpoint of the study (Fig. 6, p-values listed in Appendix A). Among the PTOA-induced limb groups, the scAAV2IL-1ra treated group had the lowest MRI OA total score (least OA progression), a statistically significant decrease in mean score as compared to the scAAV2IL-1ra/scAAV2IGF-I treated group (p-value = 0.0004). The scAAV2IL-1ra treated group showed an effect size of − 0.46 relative to the saline control group, indicating a *relatively moderate positive effect* (less PTOA progression compared with saline). In contrast, the scAAV2IL-1ra/scAAV2IGF-I treated group had an effect size of 0.95, representing a *large negative effect* (greater PTOA progression compared with saline).

Mean scores for synovial effusion, joint capsule thickness, and third carpal sclerosis were similar between PTOA-induced groups. Scores for synovial proliferation, joint capsule enthesopathy, and radial carpal sclerosis were lowest in the scAAV2IL-1ra treated group as compared to the other treated groups, although these differences were not statistically significant (data for individual MRI scoring metrics not shown). Notably, the scAAV2IL-1ra treated group was the only treated group that did not exhibit a statistically significant increase in bone edema score (greater edema) relative to the non-OA sham control group. Representative MRIs highlighting bone marrow lesions (edema) are shown in Fig. 7B.

Gross and Histological Examination

Mean cartilage erosion total scores from gross examination of the carpal bones were similar between the scAAV2IL-1ra treated and saline control group, while the scAAV2IL-1ra/scAAV2IGF-I treated group demonstrated a higher average score (worse PTOA progression) (Fig. 8A). All 3 groups that received PTOA induction showed a statistically significant increase in cartilage erosion total score as compared to the non-OA sham control, with no significant differences found between treated groups (p-values listed in Supplementary Materials). Effect size between the scAAV2IL-1ra treated group and saline control was near zero (no difference), while effect size between the scAAV2IL-1ra/scAAV2IGF-I treated group and saline control was 0.57, indicating a *medium negative effect* (greater cartilage erosion). Representative images from gross examination highlighting cartilage erosion are shown in Fig. 9A.

While gross examination of cartilage had similar scores between scAAV2IL-1ra and saline control groups, histological grading of articular cartilage revealed some differences. Total summed scores for cartilage histology were lower (less OA progression at the cellular level) in the scAAV2IL-1ra treated group as compared to both the saline control and scAAV2IL-1ra/scAAV2IGF-I treated joints (Fig. 8B). Effect size between the scAAV2IL-1ra treated joints and the saline control joints was − 1.00, indicating a *very large positive effect* (much less OA progression for scAAV2IL-1ra treated joints at the cellular level); while effect size between the scAAV2IL-1ra/scAAV2IGF-I treated joints and the saline control joints was

– 0.46, indicating a only a *medium positive effect*. Comparing cartilage histology total scores for the radial carpal bone alone (site of osteochondral chip fragment), the saline control joints had the greatest mean score (most OA progression at the cellular level), and was the only group to show a statistically significant increase (worse) in mean total score as compared to the non-OA sham control (p-value = 0.0298, mean total cartilage histology scores for individual carpal bones provided in Supplemental Material). Representative photomicrographs of the radial carpal cartilage sections scored are shown in Fig. 9B.

Mean synovium inflammation total scores from gross examination were lowest (least OA progression) in the scAAV2IL-1ra treated joints as compared to other joints, which was the only treated group that did not demonstrate a statistically significant increase in mean total synovial inflammation score as compared to the non-OA sham control joints (Fig. 8C). Notably, the effect size between the scAAV2IL-1ra treated joints and the saline control was – 0.91, indicating a *large positive effect* (much lower synovium inflammation). Opposite this the effect size between the scAAV2IL-1ra/scAAV2IGF-I treated group and the saline control was 0.39, a *small negative effect* (greater synovium inflammation). Representative images from gross examination highlighting synovial inflammation are shown in Fig. 9A.

Similar to the cartilage scoring, histological grading of synovium samples had differing results from gross examination. Total summed scores for synovium samples were lowest (least OA progression at the cellular level) in the saline control group as compared to all other groups, although no statistically significant differences in mean total summed score were found between any groups (Fig. 8D). The scAAV2IL-1ra and scAAV2IL-1ra/scAAV2IGF-I treated group had similar, higher mean total summed scores (greater OA progression at the cellular level). Effect sizes between both of these groups and the saline control indicated a *moderate negative effect* (greater OA progression at the cellular level, effect sizes = 0.62 & 0.64 for scAAV2IL-1ra and scAAV2IL-1ra/scAAV2IGF-I treated groups respectively). Individual scoring metrics for synovial histology were similar between groups, with the exception of higher synovial cellular infiltration scores (more cellular infiltration) in the scAAV2IL-1ra and scAAV2IL-1ra/scAAV2IGF-I treated groups as compared to the saline and non-OA controls (no statistically significant differences, scores for individual metrics not shown).

(A) The scAAV2IL-1ra/scAAV2IGF-I treated group had the highest cartilage (worst) erosion total score (most OA progression) from gross examination, while the scAAV2IL-1ra treated and saline control groups had similar, lower cartilage erosion total scores. All three treated groups had a statistically significant increase in cartilage erosion total score as compared to the non-OA sham control group (p-values listed in Supplementary Materials). **(B)** Total cartilage histological scores summed from the five carpal bones sampled (radial, 2nd, 3rd, 4th and ulnar carpals). The scAAV2IL-1ra treated group showed the lowest mean summed scores (least OA progression) of the three treated groups and was the only treated group that did not show a statistically significant increase in total summed score as compared to the non-OA sham control group. **(C)** The scAAV2IL-1ra treated group had the lowest synovium inflammation total score (least OA progression) as graded via gross examination of the groups that received PTOA induction; displaying a statistically significant decrease in score as compared to the

scAAV2IL-1ra/scAAV2IGF-I treated group (p-value = 0.0296). Both the scAAV2IL-1ra/scAAV2IGF-I treated and saline control groups had a statistically significant increase in synovium inflammation total score as compared to the non-OA sham control group (p-values = 0.0001 & 0.0046 respectively). **(D)** Total synovium histological scores summed from the three joint locations sampled (center, medial, and lateral). The saline control group had a slightly lower mean total summed score as compared to the other treated groups, although no statistically significant differences were found between any groups. All data displayed as mean +/- standard error.

Discussion

We report the results of an *in vivo* gene therapy study designed to determine the effects of scAAV2IL-1ra either alone or in combination with scAAV2IGF-I to treat PTOA in a well-established equine PTOA model. While this model is typically taken out to 10 weeks post-PTOA induction, this study was successfully taken out 16 weeks with no significant adverse effects. Successful surgical induction of PTOA in the middle carpal joint was confirmed by multiple outcome measures, including increased lameness, radiologic and MRI evidence of osteoarthritis, and gross and microscopic changes consistent with OA progression. Following treatment administration, immunological assays confirmed that both scAAV2IL-1ra and scAAV2IGF-I increased the levels of their respective therapeutic proteins in the synovial fluid of joints injected with the gene therapeutic vectors, in line with the results from our previous *in vitro* and *in vivo* studies utilizing these vectors [43–45, 70].

Similar to our previous studies, the scAAV2IL-1ra vector resulted in significantly elevated IL-1ra levels in all treated joints in the scAAV2IL-1ra and scAAV2IL-1ra/scAAV2IGF-I treated groups. Expression profiles varied per limb, with IL-1ra levels in the joint primarily peaking in the initial 4 weeks after treatment injection. Peak IL-1ra levels in the scAAV2IL-1ra treated group appeared subject-dependent, ranging from 10 to 175 ng/mL. A previous pilot study from our group reported an average intra-articular IL-1ra concentration ~ 300 ng/mL at Day 42 in the synovial fluid of middle carpal joints, although sample size was much lower in the previous study (n = 2 in previous vs n = 8 in the present study) [45]. Another group utilizing a 5 x 10^{11} vg dose of a similar scAAV-IL-1ra therapeutic (scAAV2.5 as opposed to scAAV2 utilized in this study) that was administered in equine carpal and metacarpophalangeal joints reported elevated IL-1ra production in the joints of n = 6 horses, with an average intra-articular IL-1ra concentration consistently around 30 ng/mL between 4–24 weeks post-injection [89]. While our study did show an average IL-1ra concentration of ~ 36 ng/mL between 2–14 weeks after treatment administration (Day 28 through study endpoint), we observed an initial peak of IL-1ra production at Days 28 and 42, which dropped off to average ~ 7 ng/mL of IL-1ra by the endpoint of the study (14 weeks post-treatment).

Consistent with our previous dosing study, PGE_2 levels (an important biomarker of inflammation in the joint) decreased after administration of the scAAV2IL-1ra treatment [44]. This statistically significant decrease in PGE_2 level was observed only in the scAAV2IL-1ra treated joints at Day 42, which coincided with the highest average IL-1ra concentration in the synovial fluid in any of the groups throughout the

study period. This decrease in PGE_2 levels was not sustained over the study period, with PGE_2 levels in the scAAV2IL-1ra treated group returning to levels similar to the other groups by Day 56. This is in contrast to our dosing study, in which PGE_2 levels decreased 14 days after administration of 5×10^{11} vg scAAV2IL-1ra and remained at a similar level through the duration of the study period. This may be due to significantly higher IL-1ra expression observed in the dosing study, indicating that a higher concentration of IL-1ra in the joint may be necessary to downregulate inflammatory pathways for a sustained period. However, the initial reduction in inflammation observed in this study may still have contributed to inhibition of OA pathogenesis, as the scAAV2IL-1ra treated group consistently had the least OA progression of the PTOA-induced groups on a large majority of the study outcome measures, including clinical evaluation (improvement in lameness), MRI scoring, gross synovial inflammation, and cartilage histological scoring.

IL-1ra levels in the scAAV2IL-1ra/scAAV2IGF-I treated group mirrored the pattern observed in the scAAV2IL-1ra treated group, with peak IL-1ra levels generally occurring within the initial 4 weeks after treatment administration. Notably, IL-1ra expression was slightly lower in the scAAV2IL-1ra/scAAV2IGF-I treated group as compared to the group treated with the scAAV2IL-1ra vector alone. IL-1ra levels peaked at a 300x fold increase in the scAAV2IL-1ra treated group (as compared to non-treated groups), while the scAAV2IL-1ra/scAAV2IGF-I treated group peaked at a 218x fold increase. Dual treatment with both the scAAV2IL-1ra and scAAV2IGF-I vectors did result in marginally elevated IGF-I levels, indicating that the use of two scAAV2 vectors to co-express multiple therapeutic proteins in equine joints is feasible; however, the overall expression of each individual transgene may be attenuated when multiple vectors are administered simultaneously. This reduced expression may be partially attributable to promoter interference, as both vectors utilize the cytomegalovirus (CMV) promoter, potentially leading to competition for host transcriptional machinery and limiting effective transcriptional output [90]. In addition, it is well documented that the CMV promoter is susceptible to transcriptional silencing in vivo [91]. We therefore cannot exclude the possibility that cellular stress induced by the dual-vector approach may exacerbate epigenetic silencing mechanisms, such as increased promoter methylation, further limiting transgene expression. These observations underscore the need for the development and implementation of more stable, in vivo–durable promoter systems to support sustained therapeutic gene expression in OA gene therapy applications. Beyond promoter-level effects, co-administration of two AAV vectors may impose additional biological constraints, including competition for viral entry pathways (such as receptor and co-receptor availability), intracellular trafficking, nuclear import, and episomal vector formation [92]. Collectively, these factors may reduce overall transduction efficiency and downstream transgene expression *in vivo*. Furthermore, the dual-vector approach inherently increases the total viral dose delivered to target cells, which may impose additional cellular stress [93]. This increased burden could alter intracellular pathways involved in protein synthesis, processing, and secretion, with each transgene potentially affected differently depending on its specific biological requirements for translation, post-translational modification, and secretion [94].

While IL-1ra levels in the scAAV2IL-1ra/scAAV2IGF-I group significantly increased, synovial IGF-I levels remained low over the duration of the study period, peaking at a ~ 4.5x fold increase as compared to IGF-I levels in non-treated joints. Synovial fluid IGF-I levels were at least slightly elevated in all 8 of the scAAV2IL-1ra/scAAV2IGF-I treated joints, indicating that low average IGF-I levels were not due to any outliers that failed to express any IGF-I. The low efficacy of the scAAV2IGF-I treatment *in vivo* sharply contrasts with previous *in vitro* findings from our group using the scAAV2IGF-I vector, suggesting the presence of an *in vivo* biological component that limits or regulates IGF-I expression [70]. In cultured equine chondrocytes, scAAV2IGF-I induced substantial elevations in IGF-I levels in the culture media, averaging approximately 600 ng/mL at a dose of 40,000 viral particles per cell. This is in stark contrast to our study, where a $5x10^{11}$ vg dose induced IGF-I levels averaging between 200–800 pg/mL in the synovial fluid, several orders of magnitude lower than the levels seen *in vitro*. Additionally, *in vitro* induction of IGF-I production promoted robust matrix formation (as seen through increased collagen type II and GAG production), while increased expression of IGF-I in the joint in this study failed to mitigate PTOA-induced damage to the articular cartilage. Interestingly, a previous study by our group showed that two separate adenoviral vectors used to express IL-1ra and IGF-I simultaneously in equine joints caused significantly increased IL-1ra expression yet no measurable increase in IGF-I expression [74]. Similar to our current findings with scAAV2IGF-I, the adenovirus promoting IGF-I expression demonstrated the ability to highly elevate IGF-I levels *in vitro*; however this effect was markedly diminished *in vivo* [95, 96]. This discrepancy highlights the importance of translational disease models, where *in vitro* efficacy may not reflect *in vivo* treatment success. It is likely that the modest increase in IGF-I expression seen in this study was not sufficient to induce anabolic changes in the PTOA-induced joints, given that other *in vivo* studies utilizing rAAV-induced IGF-I expression to treat osteochondral defects in large animal models have observed significant pro-anabolic changes [66, 67, 69]. It is also important to note that IGF-I, unlike IL-1ra, is synthesized as a pre-pro-protein and requires multiple post-translational processing steps to generate the mature, secreted form [94]. These additional requirements, including signal peptide cleavage, propeptide processing, and regulated secretion, may further constrain efficient IGF-I production *in vivo*, particularly under conditions of increased cellular burden or competition for translational and secretory machinery. As a result, IGF-I expression and secretion may be more susceptible than IL-1ra to attenuation in the context of dual-vector administration.

Surprisingly, the scAAV2IL-1ra/scAAV2IGF-I treated group did not mitigate PTOA progression nearly as well as the group treated with scAAV2IL-1ra alone. Outcome measures across the study, including clinical evaluation (improvement in lameness), MRI scoring, gross evaluation, and histological evaluation repeatedly demonstrated that the scAAV2IL-1ra/scAAV2IGF-I treated group displayed greater features of PTOA progression than the scAAV2IL-1ra treated group. We postulate that the increased PTOA progression observed in the scAAV2IL-1ra/scAAV2IGF-I treated group is likely due to a detrimental dose-related, vector-induced immune response in the joint. Here, we provide evidence that NAb formation in response to AAV2 injection appears strongly dose dependent in equine joints, with NAb titers in the scAAV2IL-1ra/scAAV2IGF-I treated group (dose=$1x10^{12}$ vg) consistently higher than in the scAAV2IL-1ra

treated group (dose=5x10^{11} vg) at both 42 and 84 days after treatment administration. This increased NAb formation in the scAAV2IL-1ra/scAAV2IGF-I group indicates that a stronger dose-related, vector-induced inflammation/immune reaction was likely present, accelerating PTOA progression as compared to the scAAV2IL-1ra treated group. This potential for rAAV-induced inflammation in the joint has been previously reported in a number of studies including our own [42, 44, 97–99]. Additionally, while PGE_2 levels in the scAAV2IL-1ra treated group dropped significantly through Day 42, PGE_2 levels did not significantly decrease in PTOA joints receiving both vectors (scAAV2IL-1ra/scAAV2IGF-I treated group). We postulate that the protective effect observed in the scAAV2IL-1ra treated group but absent in the scAAV2IL-1ra/scAAV2IGF-I treated group may be at least partially attributable to a dose-related, vector-induced immune response resulting from the increased vector burden in the scAAV2IL-1ra/scAAV2IGF-I treated group.

While this scAAV2IL-1ra/scAAV2IGF-I treatment was unable to attenuate disease progression in equine joints, we believe this is not necessarily reflective of a flaw in the treatment approach. The therapeutic potential of combining an anti-inflammatory and a pro-anabolic factor to treat OA was recently investigated in a rat knee-osteoarthritis model, where a combination of scAAV-IL-1ra (anti-inflammatory) and scAAV-SOX9 (pro-anabolic) was shown to significantly alleviate cartilage destruction and synovial inflammation as compared to either singular scAAV treatment alone [73]. Considering the positive results of a combination treatment in rat OA joints along with the efficacy of IGF-I to repair cartilage and promote a pro-anabolic environment within the joint in several large animal models [66–69], we believe that an IL-1ra/IGF-I co-delivery approach to treating OA is viable, however therapeutic protein cassettes should be combined into a single scAAV vector to avoid increased vector dose and the subsequent associated viral/inflammatory burden observed in the scAAV2IL-1ra/scAAV2IGF-I treated group in this study. The suboptimal disease attenuation observed here in the scAAV2IL-1ra/scAAV2IGF-I treated group underscores the critical need for more efficient vector systems capable of achieving clinically relevant levels of therapeutic protein expression at lower viral dosages, a theme now frequently observed in multiple human clinical trials [100].

A major limitation of this study was the relatively small sample size, which, despite being justified by an a priori power calculation, may have limited the ability to detect greater treatment effects. The variability between horses across outcome measures in this study reflects biological diversity yet may have potentially confounded the interpretation of treatment responses. Another variable in our study that requires further study is the potential relationship of putative pre-existing Abs to AAV vector efficacy. Although exposure to parvoviruses in equine are known (i.e. EqPV-H), cross reactivity to the human parvovirus B19 and AAV which only infect humans and primates has not been documented [101]. The horses utilized in this study were assigned to treatment groups without being tested for pre-existing or cross reacting AAV2 NAb levels. Eventual analysis of pre-existing serum identified NAb inhibition activity that showed moderate to strong correlation with total therapeutic protein produced over the study period (see Supplementary Fig. 7). Future preclinical and clinical studies utilizing AAV2 should consider

screening and excluding individuals with higher titers of pre-existing or cross reacting AAV2 NAbs due to their potential effect on treatment efficacy.

Conclusion

The results of this study suggest that co-expression of multiple therapeutic proteins to treat OA/PTOA in equine joints using two separate scAAV2 vectors is viable, however the increased viral load associated with the use of multiple vectors may cause a detrimental dose-related, vector-induced immune response in the joint. An important finding of this study was that a dose of $5x10^{11}$ vg scAAV2IL-1ra had attenuating effects on PTOA progression when administered alone, while a combination dose of $5x10^{11}$ vg scAAV2IL-1ra + $5x10^{11}$ vg scAAV2IGF-I was not sufficient to attenuate PTOA progression or induce pro-anabolic changes in the joint. The authors conclude that a scAAV-induced IL-1ra/IGF-I combination treatment may have potential to address both inflammation and tissue degradation in OA joints, however more efficient AAV vectors are needed to induce therapeutically relevant levels of IL-1ra and IGF-I in the joint without increasing the total viral load, while further *in vivo* studies should integrate screening for pre-existing NAbs. Despite the inability of the combined treatment approach to attenuate PTOA progression, scAAV2IL-1ra treatment alone demonstrated exciting promise in decreasing the inflammatory component of PTOA, which resulted in attenuation of many outcomes of PTOA in this equine preclinical model. Considering this model is highly relevant to human PTOA, these results encourage the pursuit of this therapy in clinical OA treatment for both horses and people.

Declarations

Ethical Approval:

All animal studies were approved and conducted in accordance with Institutional Animal Care and Use Committee (IACUC #1517) and Animal Care and Use Review Office protocol OR170376.e002 guidelines.

Competing Interests:

The authors declare no competing interests.

Funding:

This study was supported by funds from the Department of Defense award W81XWH1810572.

Author Contribution

JHO, PT, JNP, and LRG conceived and/or designed the work that led to the submission, acquired data, and/or played an important role in interpreting the results. AMH provided guidance with the statistical

analysis. JHO and LRG drafted the manuscript. PT, JNP, MFB, KAS, LC, LMP, LS, CRC, CWM, RJS, BBN and LRG were involved in revisions and approval of the final version. All authors have read and approved the final version and agree to be accountable for all aspects of the work in ensuring that questions related to the accuracy or integrity of any part of the work are appropriately investigated and resolved.

Acknowledgement

The authors acknowledge the assistance of the Orthopaedic Research Center preclinical trials equine care team, Jennifer Daniels, Natalie Lombard, Ryan Shelton, and barn crew members for their care of the horses within this study.

Data Availability

The data that support the findings of this study are available from the corresponding author Dr. Laurie Goodrich upon reasonable request.

References

1. Xu S, et al. Trends in prevalence of arthritis by race among adults in the United States, 2011–2018. BMC Public Health. 2024;24(1):1507.
2. Network GB. o.D.C., *Global burden of disease study 2019 (GBD 2019) results.* Seattle, 2020.
3. Torio CM, Moore BJ. Statistical brief# 204 national inpatient hospital costs: The most expensive conditions by payer, 2013. Hcup. 2016;204:1–15.
4. Rivera JC, et al. Posttraumatic osteoarthritis caused by battlefield injuries: the primary source of disability in warriors. JAAOS-Journal Am Acad Orthop Surg. 2012;20:S64–9.
5. Neundorf RH, et al. Determination of the prevalence and severity of metacarpophalangeal joint osteoarthritis in Thoroughbred racehorses via quantitative macroscopic evaluation. Am J Vet Res. 2010;71(11):1284–93.
6. Ross MW, Dyson SJ. Diagnosis and Management of Lameness in the Horse. Elsevier Health Sciences; 2010.
7. Goodrich LR, Nixon AJ. Medical treatment of osteoarthritis in the horse–a review. Vet J. 2006;171(1):51–69.
8. McIlwraith C, Frisbie D, Kawcak C. The horse as a model of naturally occurring osteoarthritis. Bone joint Res. 2012;1(11):297–309.
9. McIlwraith CW, et al. Joint disease in the horse. Elsevier Health Sciences; 2015.
10. Ji X, Zhang H. Current strategies for the treatment of early stage osteoarthritis. Front Mech Eng. 2019;5:57.

11. Geng R, et al. Knee osteoarthritis: Current status and research progress in treatment. Experimental therapeutic Med. 2023;26(4):1–11.
12. Roth SH. Nonsteroidal anti-inflammatory drug gastropathy: new avenues for safety. Clin Interv Aging, 2011: pp. 125–31.
13. Melchiorri D, et al. Regulatory evaluation of Glybera in Europe—two committees, one mission. Nat Rev Drug Discovery. 2013;12(9):719–719.
14. Food U, Administration D. FDA approves novel gene therapy to treat patients with a rare form of inherited vision loss. US Dep Heal Hum Serv; 2017.
15. Food U. *Drug Administration (FDA):'FDA approves innovative gene therapy to treat pediatric patients with spinal muscular atrophy, a rare disease and leading genetic cause of infant mortality| FDA'*, 2019.
16. Agency EM. *Upstaza (eladocagene exuparvovec).*
17. Administration US. F.a.D., *ELEVIDYS (delandistrogene moxeparvovec-rokl).*
18. Food U, Administration D. *Roctavian.* US Food and Drug Administration. USA: Silver Spring, MY; 2023.
19. Food U, Administration D. *Hemgenix*. 2023.
20. Food, Administration D. *Beqvez (fidanacogene elaparvovec-dzkt), Summary Basis for Regulatory Action*.
21. Wei H, Xiao W, Dai J. China's first approved gene therapy for hemophilia B: A new era for global AAV-based treatments. Mol Ther. 2025;33(6):2312–3.
22. De la Vega RE, et al. A phase 1 clinical trial shows safe, sustained, AAV-mediated expression of IL-1Ra in the human osteoarthritic knee joint. Sci Transl Med. 2025;17(801):eadu9804.
23. ClinicalTrials.Gov. *A Study Evaluating the Safety, Tolerability, and Activity of ICM-203 in Subjects With Knee Osteoarthritis.*; Available from: https://clinicaltrials.gov/study/NCT05454566
24. ClinicalTrials.Gov. *A Study Evaluating the Safety, Tolerability, and Range of Biologically Active Doses of ICM-203 in Mild to Moderate Knee Osteoarthritis*. Available from: https://clinicaltrials.gov/study/NCT04875754
25. ClinicalTrials.Gov. *ART-I02 in Patients With Rheumatoid Arthritis With Inflamed Wrists*. Available from: https://clinicaltrials.gov/study/NCT03445715
26. ClinicalTrials.Gov. *A Single Dose Clinical Trial to Study the Safety of ART-I02 in Patients With Arthritis*. Available from: https://clinicaltrials.gov/study/NCT02727764
27. ClinicalTrials.Gov. *Phase 1 Dose Escalation Study of Intra-Articular Administration of tgAAC94*. Available from: https://clinicaltrials.gov/study/NCT00617032?term=NCT00617032&rank=1
28. ClinicalTrials.Gov. *Study of Intra-articular Delivery of tgAAC94 in Inflammatory Arthritis Subjects*. Available from: https://clinicaltrials.gov/study/NCT00126724?term=NCT00126724&rank=1
29. Yao Q, et al. Osteoarthritis: pathogenic signaling pathways and therapeutic targets. Signal Transduct Target therapy. 2023;8(1):56.

30. Li X, et al. New treatment for osteoarthritis: Gene therapy. Precision Clin Med. 2023;6(2):pbad014.
31. Anderson DD, et al. Post-traumatic osteoarthritis: improved understanding and opportunities for early intervention. J Orthop Res. 2011;29(6):802–9.
32. Estrada McDermott J, et al. Role of innate immunity in initiation and progression of osteoarthritis, with emphasis on horses. Animals. 2021;11(11):3247.
33. Goldring MB, Otero M. Inflammation in osteoarthritis. Curr Opin Rheumatol. 2011;23(5):471–8.
34. Sanchez-Lopez E, et al. Synovial inflammation in osteoarthritis progression. Nat Rev Rheumatol. 2022;18(5):258–75.
35. Hedbom E, Häuselmann H. Molecular aspects of pathogenesis in osteoarthritis: the role of inflammation. Cell Mol Life Sci CMLS. 2002;59:45–53.
36. Xu D, et al. MMP-1 overexpression induced by IL-1β: possible mechanism for inflammation in degenerative lumbar facet joint. J Orthop Sci. 2013;18(6):1012–9.
37. Rousset F, et al. IL-1β mediates MMP secretion and IL-1b neosynthesis via upregulation of p22phox and nox4 activity in human articular chondrocytes. Osteoarthr Cartil. 2014;22:S173.
38. Fan Z, et al. Freshly isolated osteoarthritic chondrocytes are catabolically more active than normal chondrocytes, but less responsive to catabolic stimulation with interleukin-1β. Arthritis Rheumatism: Official J Am Coll Rheumatol. 2005;52(1):136–43.
39. Elliott S, et al. The triterpenoid CDDO inhibits expression of matrix metalloproteinase-1, matrix metalloproteinase-13 and Bcl-3 in primary human chondrocytes. Arthritis Res Ther. 2003;5:1–7.
40. Kobayashi M, et al. Role of interleukin-1 and tumor necrosis factor α in matrix degradation of human osteoarthritic cartilage. Arthritis Rheumatism: Official J Am Coll Rheumatol. 2005;52(1):128–35.
41. Bondeson J, et al. Adenoviral gene transfer of the endogenous inhibitor IkappaBalpha into human osteoarthritis synovial fibroblasts demonstrates that several matrix metalloproteinases and aggrecanases are nuclear factor-kappaB-dependent. J Rhuematol. 2007;34(3):523–33.
42. Goodrich LR, et al. IL-1ra gene therapy in equine osteoarthritis improves physiological, anatomical, and biological outcomes of joint degeneration. J Am Vet Med Assoc. 2024;1(aop):1–12.
43. Goodrich LR et al. Optimization of scAAVIL-1ra in vitro and in vivo to deliver high levels of therapeutic protein for treatment of osteoarthritis. Mol Therapy-Nucleic Acids, 2013. 2.
44. Thampi P, et al. A pilot study to determine the optimal dose of scAAVIL-1ra in a large animal model of post-traumatic osteoarthritis. Gene Ther. 2023;30(12):792–800.
45. Goodrich L, et al. scAAVIL-1ra dosing trial in a large animal model and validation of long-term expression with repeat administration for osteoarthritis therapy. Gene Ther. 2015;22(7):536–45.
46. Zhang P, et al. Exogenous expression of IL-1Ra and TGF-β1 promotes in vivo repair in experimental rabbit osteoarthritis. Scand J Rheumatol. 2015;44(5):404–11.
47. Senter R, et al. Efficacy and safety of FX201, a novel intra-articular IL-1Ra gene therapy for osteoarthritis treatment, in a rat model. Hum Gene Ther. 2022;33(9–10):541–9.

48. Wang F, et al. IL-1β receptor antagonist (IL-1Ra) combined with autophagy inducer (TAT-Beclin1) is an effective alternative for attenuating extracellular matrix degradation in rat and human osteoarthritis chondrocytes. Volume 21. Arthritis research & therapy; 2019. pp. 1–14.
49. Rutgers M, et al. Cytokine profile of autologous conditioned serum for treatment of osteoarthritis, in vitro effects on cartilage metabolism and intra-articular levels after injection. Volume 12. Arthritis research & therapy; 2010. p. R114. 3.
50. Chevalier X, et al. Intraarticular injection of anakinra in osteoarthritis of the knee: a multicenter, randomized, double-blind, placebo-controlled study. Volume 61. Arthritis Care & Research; 2009. pp. 344–52. 3.
51. Hung GL, et al. Suppression of intra-articular responses to interleukin-1 by transfer of the interleukin-1 receptor antagonist gene to synovium. Gene Ther. 1994;1(1):64–9.
52. Wang HJ, et al. Suppression of experimental osteoarthritis by adenovirus-mediated double gene transfer. Chin Med J. 2006;119(16):1365–73.
53. Gouze E, et al. Lentiviral-mediated gene delivery to synovium: potent intra-articular expression with amplification by inflammation. Mol Ther. 2003;7(4):460–6.
54. Frisbie DD, et al. Treatment of experimental equine osteoarthritis by in vivo delivery of the equine interleukin-1 receptor antagonist gene. Gene Ther. 2002;9(1):12–20.
55. Evans CH, et al. Gene transfer to human joints: progress toward a gene therapy of arthritis. Proc Natl Acad Sci USA. 2005;102(24):8698–703.
56. Wehling P, et al. Clinical responses to gene therapy in joints of two subjects with rheumatoid arthritis. Hum Gene Ther. 2009;20(2):97–101.
57. Weimer A, et al. Benefits of recombinant adeno-associated virus (rAAV)-mediated insulinlike growth factor I (IGF-I) overexpression for the long-term reconstruction of human osteoarthritic cartilage by modulation of the IGF-I axis. Mol Med. 2012;18:346–58.
58. Madry H, et al. Gene transfer of a human insulin-like growth factor I cDNA enhances tissue engineering of cartilage. Hum Gene Ther. 2002;13(13):1621–30.
59. Cucchiarini M, Madry H. Overexpression of human IGF-I via direct rAAV-mediated gene transfer improves the early repair of articular cartilage defects in vivo. Gene Ther, 2014.
60. Madry H, et al. Cartilage constructs engineered from chondrocytes overexpressing IGF-I improve the repair of osteochondral defects in a rabbit model. Eur Cells Mater. 2013;25:229–47.
61. Leng P, et al. Reconstruct large osteochondral defects of the knee with hIGF-1 gene enhanced Mosaicplasty. Knee. 2012;19(6):804–11.
62. Aguilar IN, et al. Customized biomaterials to augment chondrocyte gene therapy. Acta Biomater. 2017;53:260–7.
63. Aguilar IN, et al. Comparison of efficacy of endogenous and exogenous IGF-I in stimulating matrix production in neonatal and mature chondrocytes. Cartilage. 2015;6(4):264–72.

64. Goodrich LR, et al. Direct adenovirus-mediated IGF-I gene transduction of synovium induces persisting synovial fluid IGF-I ligand elevations. Gene Ther. 2006;13(17):1253–62.
65. Goodrich LR, et al. Genetic modification of chondrocytes with insulin-like growth factor-1 enhances cartilage healing in an equine model. J Bone Joint Surg Br. 2007;89(5):672–85.
66. Peifer C, et al. Locally Directed Recombinant Adeno-Associated Virus–Mediated IGF-1 Gene Therapy Enhances Osteochondral Repair and Counteracts Early Osteoarthritis In Vivo. Am J Sports Med. 2024;52(5):1336–49.
67. Maihöfer J, et al. Hydrogel-Guided, rAAV-Mediated IGF-I Overexpression Enables Long-Term Cartilage Repair and Protection against Perifocal Osteoarthritis in a Large-Animal Full-Thickness Chondral Defect Model at One Year In Vivo. Adv Mater. 2021;33(16):2008451.
68. Ortved K, et al. Humoral and cell-mediated immune response, and growth factor synthesis after direct intraarticular injection of rAAV2-IGF-I and rAAV5-IGF-I in the equine middle carpal joint. Hum Gene Ther. 2015;26(3):161–71.
69. Ortved KF, et al. Implantation of rAAV5-IGF-I transduced autologous chondrocytes improves cartilage repair in full-thickness defects in the equine model. Mol Ther. 2015;23(2):363–73.
70. Hemphill D, et al. Adeno-associated virus gene therapy vector scAAVIGF-I for transduction of equine articular chondrocytes and RNA-seq analysis. Osteoarthr Cartil. 2016;24(5):902–11.
71. Cucchiarini M, et al. Remodelling of human osteoarthritic cartilage by FGF-2, alone or combined with Sox9 via rAAV gene transfer. J Cell Mol Med. 2009;13(8b):2476–88.
72. Tao K, et al. Co-overexpression of TGF-β and SOX9 via rAAV gene transfer modulates the metabolic and chondrogenic activities of human bone marrow-derived mesenchymal stem cells. Stem Cell Res Ther. 2016;7:1–12.
73. Zhou K et al. *Co-delivery of IL-1Ra and SOX9 via AAV inhibits inflammation and promotes cartilage repair in surgically induced osteoarthritis animal models.* Gene Therapy, 2025: pp. 1–12.
74. Morisset S, et al. IL-1ra/IGF-1 gene therapy modulates repair of microfractured chondral defects. Clin Orthop Relat Research®. 2007;462:221–8.
75. Liu Q, et al. Neutralizing antibodies against AAV2, AAV5 and AAV8 in healthy and HIV-1-infected subjects in China: implications for gene therapy using AAV vectors. Gene Ther. 2014;21(8):732–8.
76. Ling C, et al. Prevalence of neutralizing antibodies against liver-tropic adeno-associated virus serotype vectors in 100 healthy Chinese and its potential relation to body constitutions. J Integr Med. 2015;13(5):341–6.
77. Van Der Marel S, et al. Neutralizing antibodies against adeno-associated viruses in inflammatory bowel disease patients: implications for gene therapy. Inflamm Bowel Dis. 2011;17(12):2436–42.
78. Wang X, et al. Seroprevalence of binding and neutralizing antibodies against 18 adeno-associated virus types in patients with neuromuscular disorders. Front Immunol. 2024;15:1450858.
79. Rapti K, et al. Neutralizing antibodies against AAV serotypes 1, 2, 6, and 9 in sera of commonly used animal models. Mol Ther. 2012;20(1):73–83.

80. Calcedo R, et al. Preexisting neutralizing antibodies to adeno-associated virus capsids in large animals other than monkeys may confound in vivo gene therapy studies. Hum gene therapy methods. 2015;26(3):103–5.
81. Frisbie DD, et al. Evaluation of polysulfated glycosaminoglycan or sodium hyaluronan administered intra-articularly for treatment of horses with experimentally induced osteoarthritis. Am J Vet Res. 2009;70(2):203–9.
82. Seabaugh KA, et al. Examining the effects of the oral supplement biota orientalis in the osteochondral fragment-exercise model of osteoarthritis in the horse. Front Veterinary Sci. 2022;9:858391.
83. Cottard V, et al. Immune response against gene therapy vectors: influence of synovial fluid on adeno-associated virus mediated gene transfer to chondrocytes. J Clin Immunol. 2004;24(2):162–9.
84. Boissier M-C, et al. Synoviocyte infection with adeno-associated virus (AAV) is neutralized by human synovial fluid from arthritis patients and depends on AAV serotype. Hum Gene Ther. 2007;18(6):525–35.
85. Andersen C, et al. A detailed macroscopic scoring system for experimental post-traumatic Osteoarthritis in the equine middle carpal joint. BMC Res Notes. 2022;15(1):226.
86. McIlwraith C, et al. The OARSI histopathology initiative–recommendations for histological assessments of osteoarthritis in the horse. Osteoarthr Cartil. 2010;18:S93–105.
87. Core Team R. R: A Language and Environment for Statistical Computing. R Foundation for Statistical Computing; 2025.
88. Frisbie DD et al. *Changes in synovial fluid and serum biomarkers with exercise and early osteoarthritis in horses.* Osteoarthritis and cartilage / OARS, Osteoarthritis Research Society, 2008. 16(10): pp. 1196 – 204.
89. Watson Levings RS, et al. Gene therapy for osteoarthritis: pharmacokinetics of intra-articular self-complementary adeno-associated virus interleukin-1 receptor antagonist delivery in an equine model. Hum gene therapy Clin Dev. 2018;29(2):90–100.
90. Andersen CR, et al. Efficient expression from one CMV enhancer controlling two core promoters. Mol Biotechnol. 2011;48(2):128–37.
91. Brooks AR et al. *Transcriptional silencing is associated with extensive methylation of the CMV promoter following adenoviral gene delivery to muscle.* The Journal of Gene Medicine: A cross-disciplinary journal for research on the science of gene transfer and its clinical applications, 2004. 6(4): pp. 395–404.
92. Ding W, et al. Intracellular trafficking of adeno-associated viral vectors. Gene Ther. 2005;12(11):873–80.
93. Xiao X, Li J, Samulski RJ. Efficient long-term gene transfer into muscle tissue of immunocompetent mice by adeno-associated virus vector. J Virol. 1996;70(11):8098–108.
94. Durzyńska J, et al. The pro-forms of insulin-like growth factor I (IGF-I) are predominant in skeletal muscle and alter IGF-I receptor activation. Endocrinology. 2013;154(3):1215–24.

95. Nixon A, et al. Gene-mediated restoration of cartilage matrix by combination insulin-like growth factor-I/interleukin-1 receptor antagonist therapy. Gene Ther. 2005;12(2):177–86.
96. Haupt JL, et al. Dual transduction of insulin-like growth factor-I and interleukin-l receptor antagonist protein controls cartilage degradation in an osteoarthritic culture model. J Orthop Res. 2005;23(1):118–26.
97. Ishihara A, Bartlett JS, Bertone AL. Inflammation and immune response of intra-articular serotype 2 adeno-associated virus or adenovirus vectors in a large animal model. Arthritis. 2012;2012(1):735472.
98. Mease PJ, et al. Safety, tolerability, and clinical outcomes after intraarticular injection of a recombinant adeno-associated vector containing a tumor necrosis factor antagonist gene: results of a phase 1/2 Study. J Rhuematol. 2010;37(4):692–703.
99. Luo S, et al. The Intra-Articular Delivery of a Low-Dose Adeno-Associated Virus-IL-1 Receptor Antagonist Vector Alleviates the Progress of Arthritis in an Osteoarthritis Rat Model. Pharmaceutics. 2024;16(12):1518.
100. Mendell JR, et al. Current clinical applications of in vivo gene therapy with AAVs. Mol Ther. 2021;29(2):464–88.
101. Tomlinson JE, et al. Tropism, pathology, and transmission of equine parvovirus-hepatitis. Volume 9. Emerging microbes & infections; 2020. pp. 651–63. 1.

Figures

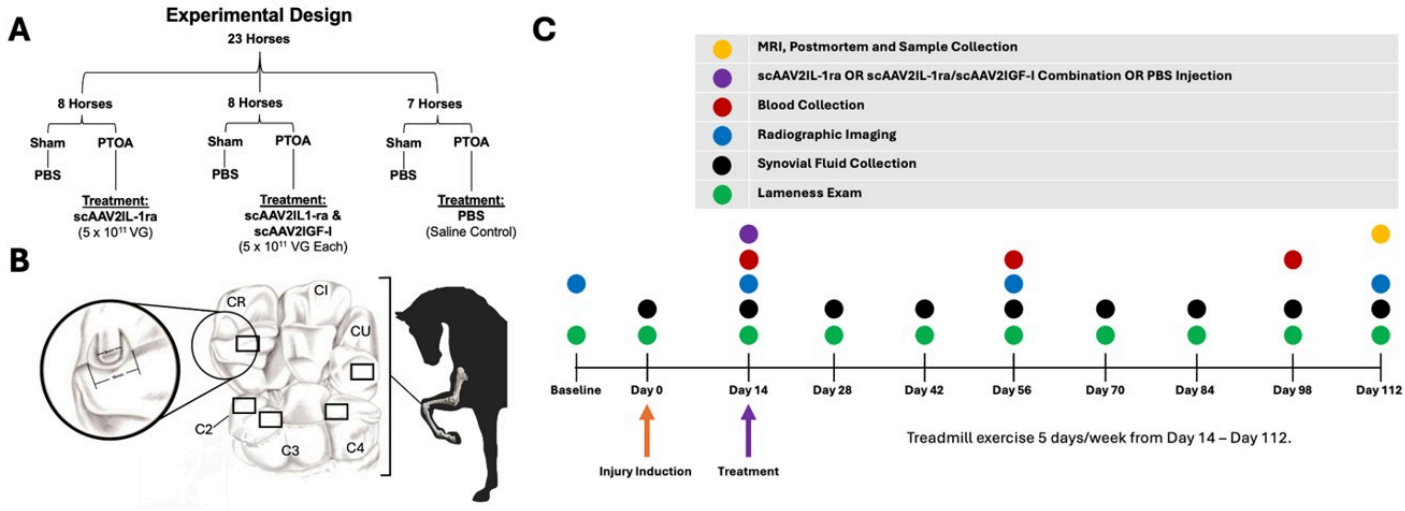


Figure 1

Experimental design, equine middle carpal joint illustration, and study timeline.

(A) Schematic of treatment and control groups, defined by the presence or absence of an osteochondral chip fragment (PTOA induction) in the equine middle carpal joint, with intra-articular administration of

scAAV2IL-1ra, combined scAAV2IL-1ra/scAAV2IGF-I, or saline treatment 14 days following surgery. **(B)**An illustration of the equine middle carpal joint indicating the area where the osteochondral chip fragment was induced (close-up view shown to the left). The empty black boxes indicate areas of the carpal bones where articular cartilage samples were taken for histology (CR-radial carpal, CU-ulnar carpal, C2-second carpal, C3-third carpal, and C4-fourth carpal). Diagram adapted from Goodrich et al, *Journal of the American Veterinary Medical Association*, 2024 with permission. **(C)** Study timeline indicating treatment administration, clinical data, and sample collection. Dots above the timeline indicate points for lameness exams, synovial fluid aspiration, blood collection, radiographs, and MRI.

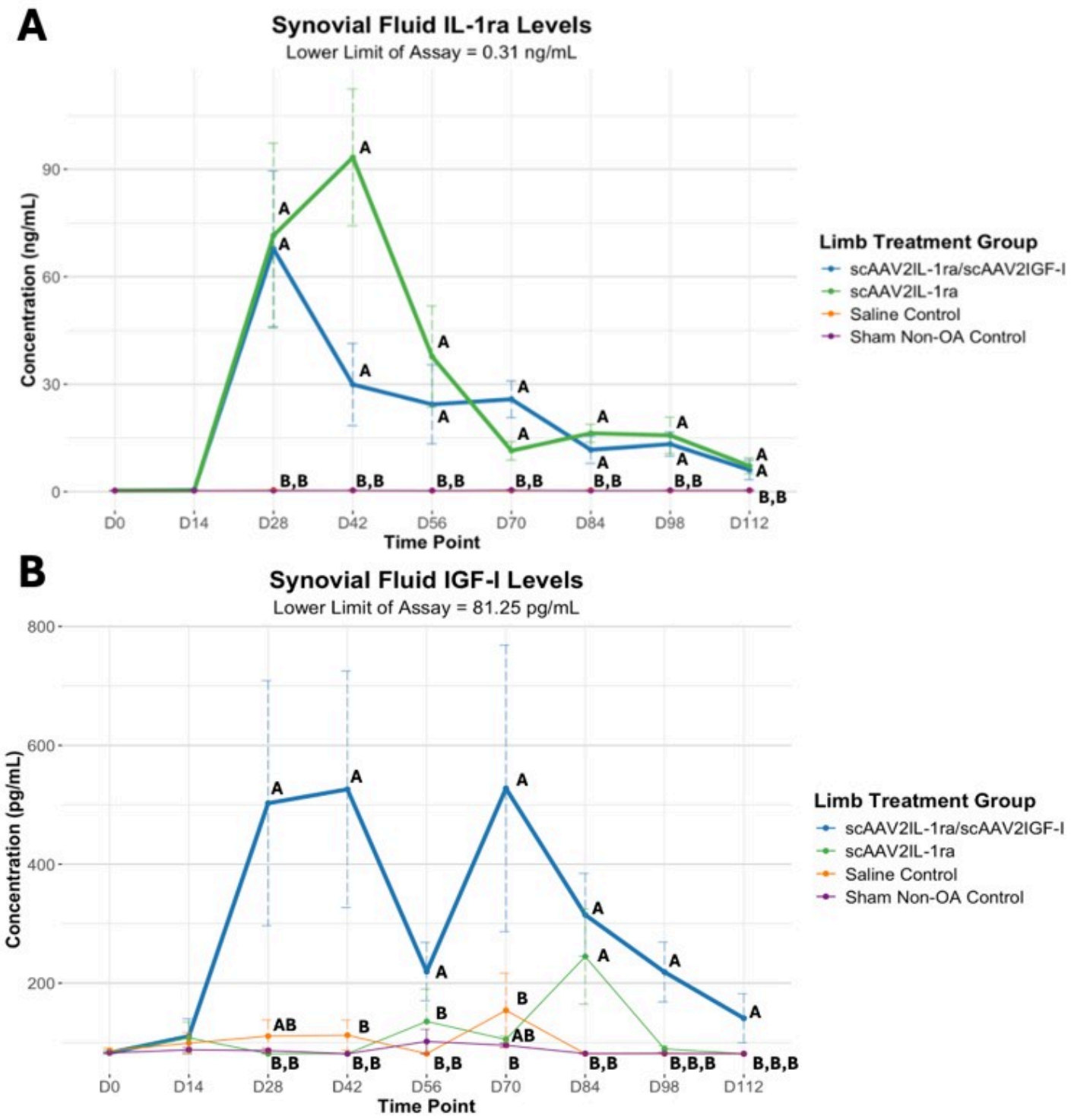


Figure 2

Mean IL-1ra (A) and IGF-I (B) levels in the synovial fluid of all joints over the study period. (A) Mean IL-1ra levels in the synovial fluid of both groups treated with the scAAV2IL-1ra vector (scAAV2IL-1ra treated group and scAAV2IL-1ra/scAAV2IGF-I treated group) were significantly increased at all time points following treatment injection at Day 14. Mean IL-1ra levels in the groups that did not receive the scAAV2IL-1ra treatment (saline control and non-OA sham control) were almost entirely below the assay

limit of detection (0.31 ng/mL) throughout the study period. **(B)** Mean IGF-I levels in the synovial fluid of the scAAV2IL-1ra/scAAV2IGF-I treated group were marginally elevated at all time points following treatment injection at Day 14. IGF-I levels in the groups that did not receive scAAV2IGF-I (scAAV2IL-1ra treated, saline control, and non-OA sham control) stayed near the lower limit of assay detection (81.25 pg/mL) throughout the study period. All data displayed as mean +/- standard error.

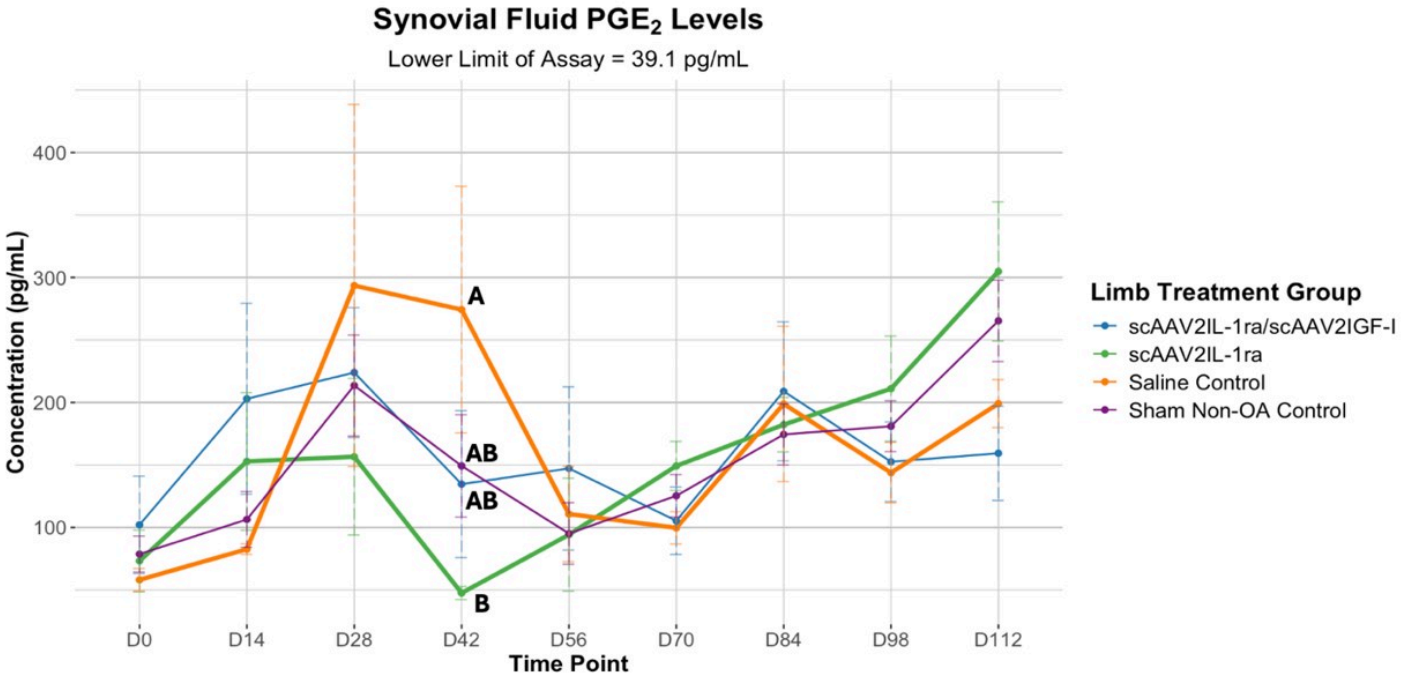


Figure 3

Mean synovial fluid PGE_2 (pg/mL) levels in all joints over the study period. Synovial fluid PGE_2 levels increased in all groups from Day 0 (PTOA induction) to Day 14 (treatment administration). After Day 14 synovial fluid PGE_2 levels remained similar throughout the remainder of the study period, with the exception of a statistically significant decrease in PGE_2 levels in the scAAV2IL-1ra treated group (bold green line) as compared to the saline control group (bold orange line) at Day 42. This decrease in PGE_2 levels in the scAAV2IL-1ra treated group at Day 42 coincided with the highest levels of IL-1ra expression observed during the study period (see Figure 2A). Data displayed as mean +/- standard error.

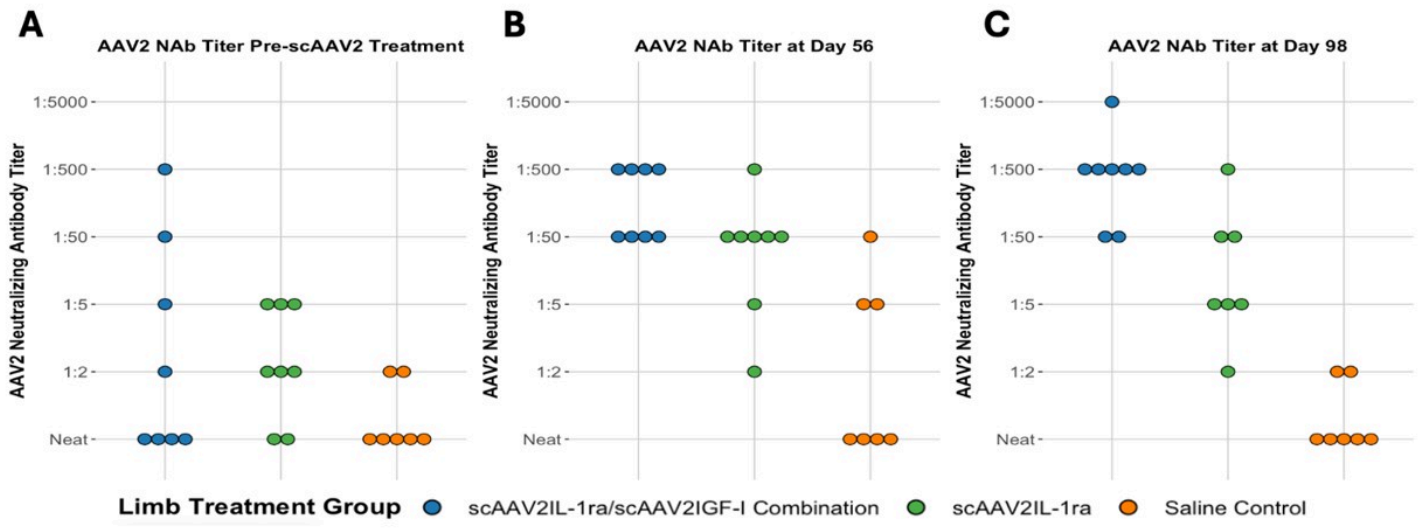


Figure 4

AAV2 serum neutralizing antibody titers per horse over the study period. (A) Pre-existing AAV2 serum NAb titers per treatment group (titers determined by serial dilution). A majority of titers in all 3 treatment groups were low pre-scAAV2 administration (neat or 1:2). **(B)** AAV2 serum NAb titers per treatment group at Day 56 (42 days post-treatment administration). NAb titers in the saline control group remained relatively low after treatment injection, with a moderate increase in NAb titers in the scAAV2IL-1ra treated group and a more profound increase in the scAAV2IL-1ra/scAAV2IGF-I treated group (suggesting greater AAV2 NAb formation in response to viral dose). **(C)** AAV2 serum NAb titers per treatment group at Day 98 (84 days post-treatment administration). NAb titers in the saline control group continued to remain low, while titers in the scAAV2IL-1ra treated group were overall lower as compared to their titers at Day 56. This is opposite to the scAAV2IL-1ra/scAAV2IGF-I treated group, which continued to demonstrate increasingly higher titers at Day 98 as compared to Day 56.

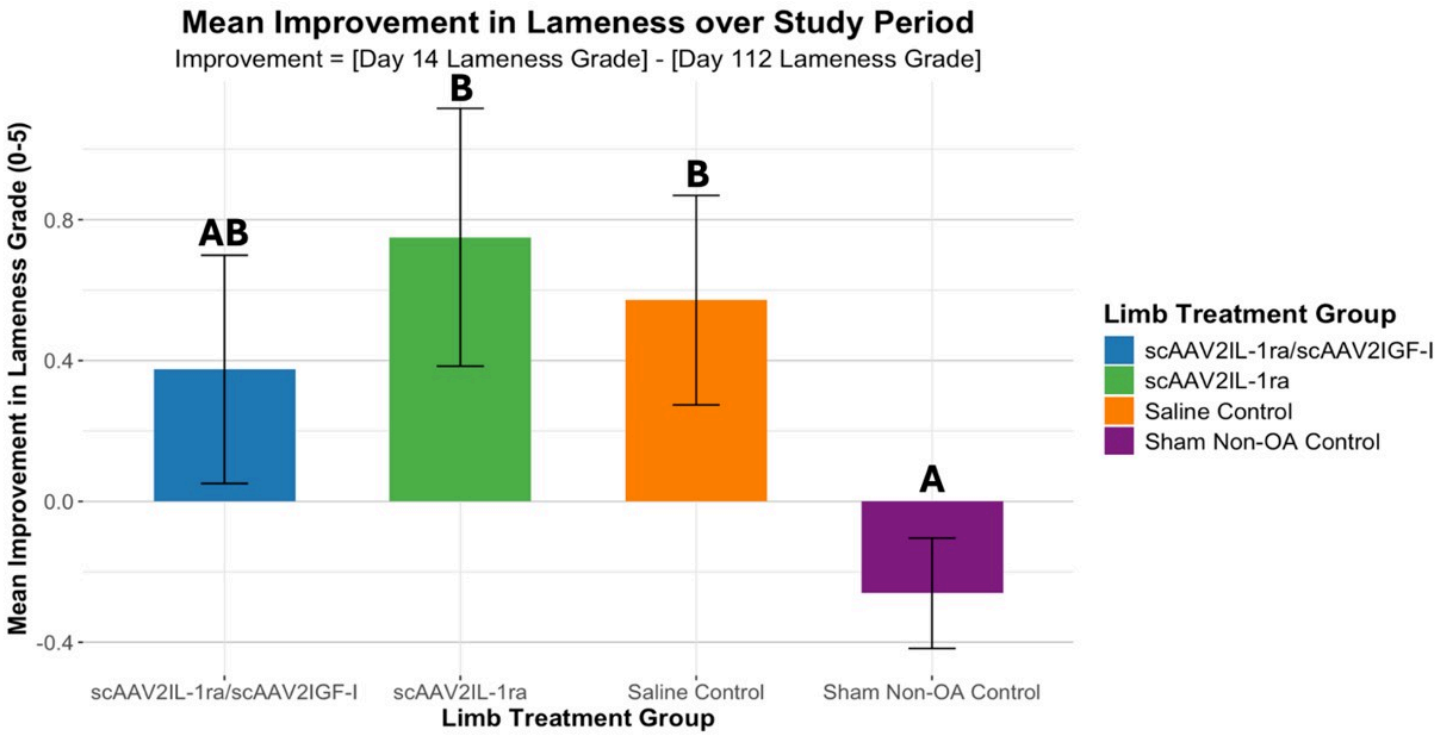


Figure 5

Mean improvement in lameness in all joints after treatment administration. Mean improvement in lameness over the study was calculated as the Day 14 lameness grade (immediately before treatment administration) minus the Day 112 lameness grade (study endpoint) for each joint. Lameness grade was typically highest at Day 14, with a greater (more positive) score in improvement in lameness indicating that the joint improved clinically over the study period. Mean improvement in lameness was highest (greatest improvement in lameness) in the scAAV2IL-1ra treated group of the three PTOA-induced groups. Improvement in lameness was negative in the non-OA sham control group, indicating that these joints became more lame over the study period. All data displayed as mean +/- standard error.

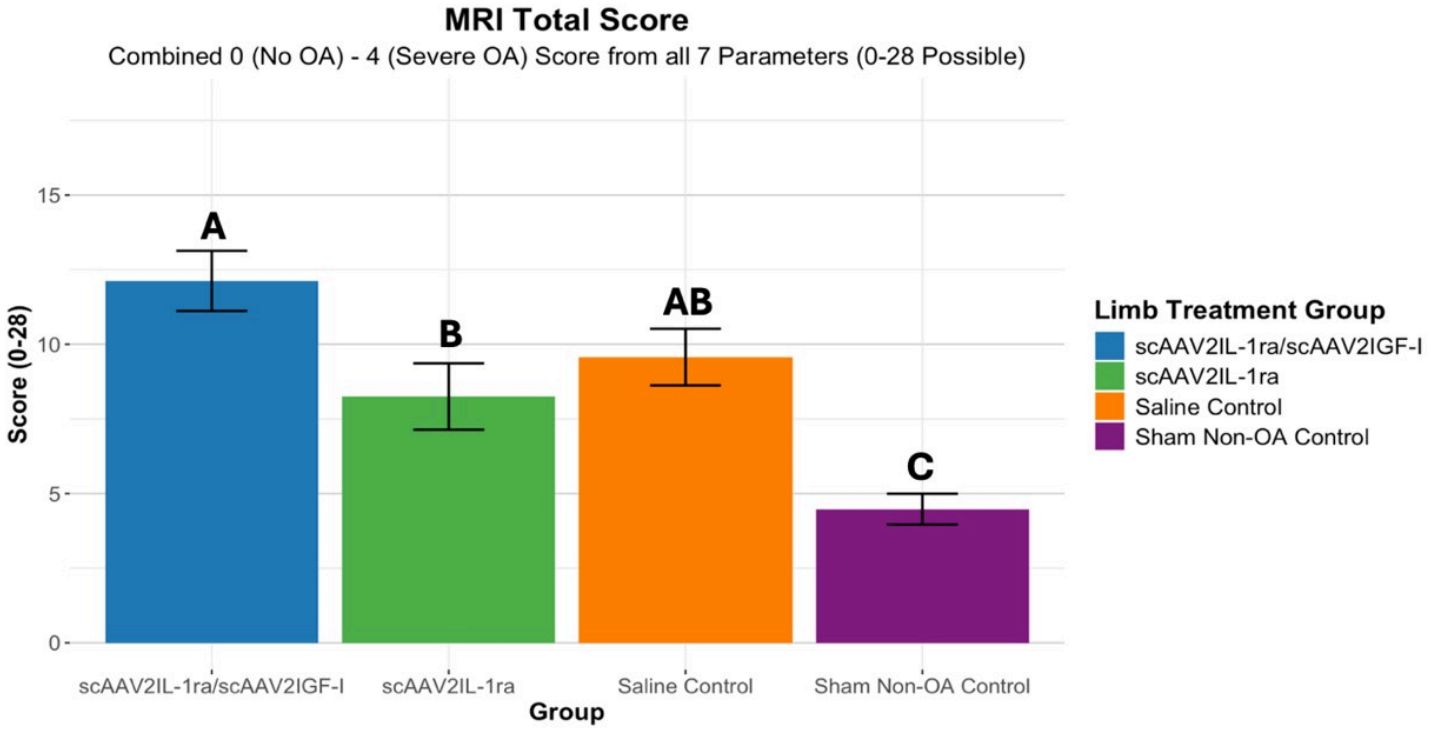


Figure 6

Effects of the scAAV2 treatments on OA progression as graded via MRI. Mean MRI OA total scores in all joints at the endpoint of the study. MRI OA total score summed the 0 (no OA) – 4 (severe OA) scores for synovial proliferation, synovial effusion, JCE, joint capsule thickness (JCT), bone edema, radial carpal sclerosis, and third carpal sclerosis. Mean MRI OA total scores showed a statistically significant increase in all of the PTOA-induced limb groups as compared to the non-OA sham control group (p-values listed in Appendix A). Of the PTOA-induced limb groups, the scAAV2IL-1ra treated group showed the lowest MRI OA total score (least PTOA progression), which was a statistically significant decrease in score as compared to the scAAV2IL-1ra/scAAV2IGF-I treated group (p-value = 0.0004). All data displayed as mean +/- standard error.

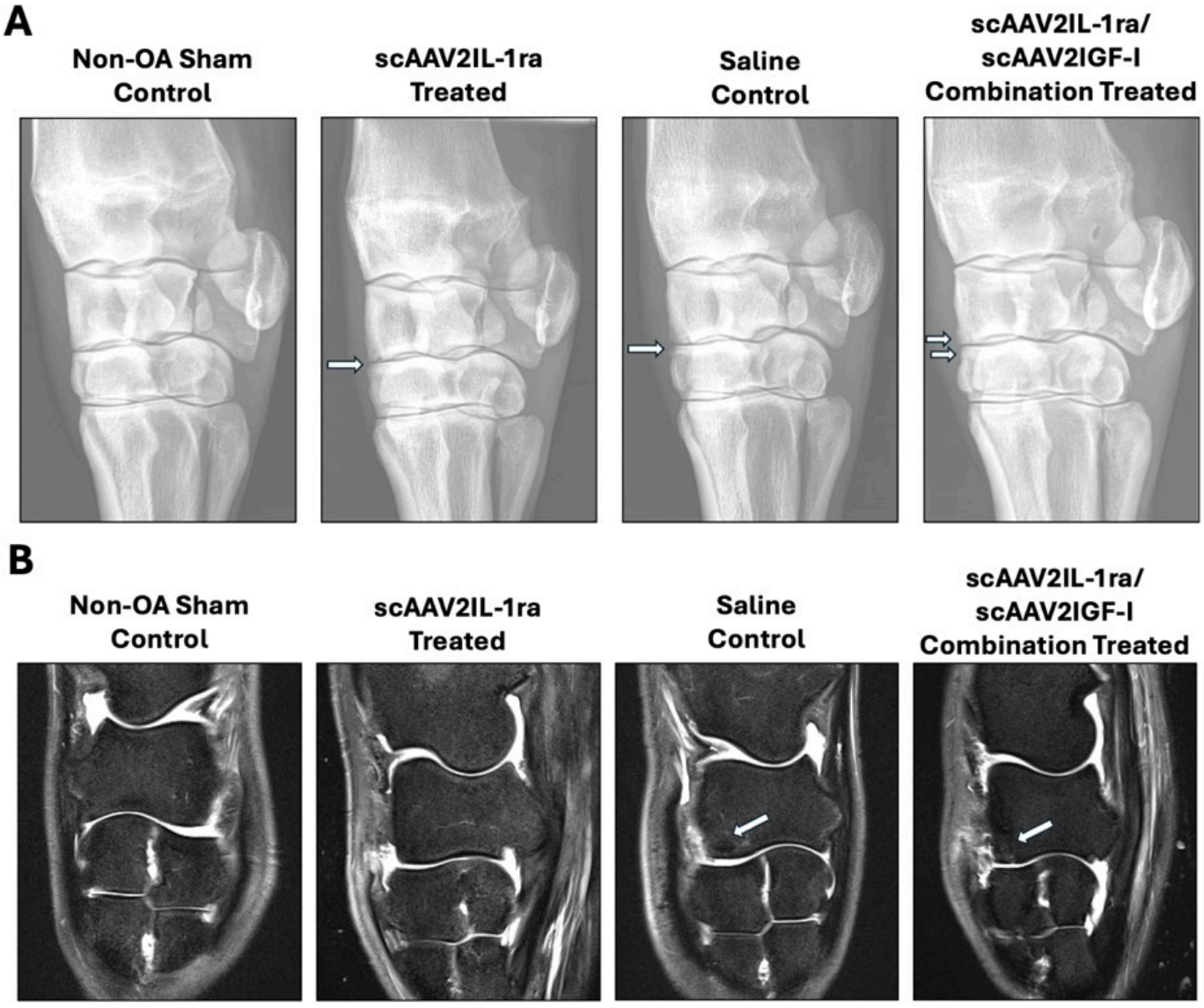


Figure 7

Representative radiographs (A) and MRIs (B) highlighting peri-articular osteophyte formation and bone marrow lesions (edema) respectively. (A) Radiographs taken at the endpoint of the study (Day 112). Radiographs are representative of peri-articular osteophyte formation score in joints, with white arrows indicating the presence of osteophytes. Non-OA sham joints showed the fewest osteophytes, followed by the scAAV2IL-1ra treated joints. The scAAV2IL-1ra/scAAV2IGF-I treated joints showed the greatest osteophyte formation of the treated groups. **(B)** MRIs taken at the endpoint of the study (Day 112). MRIs are representative of bone marrow lesions (edema) in the joint, with white arrows indicating areas of lesions. Non-OA sham joints showed the least bone edema, followed by the scAAV2IL-1ra treated joints. The scAAV2IL-1ra/scAAV2IGF-I treated joints typically showed the greatest bone edema.

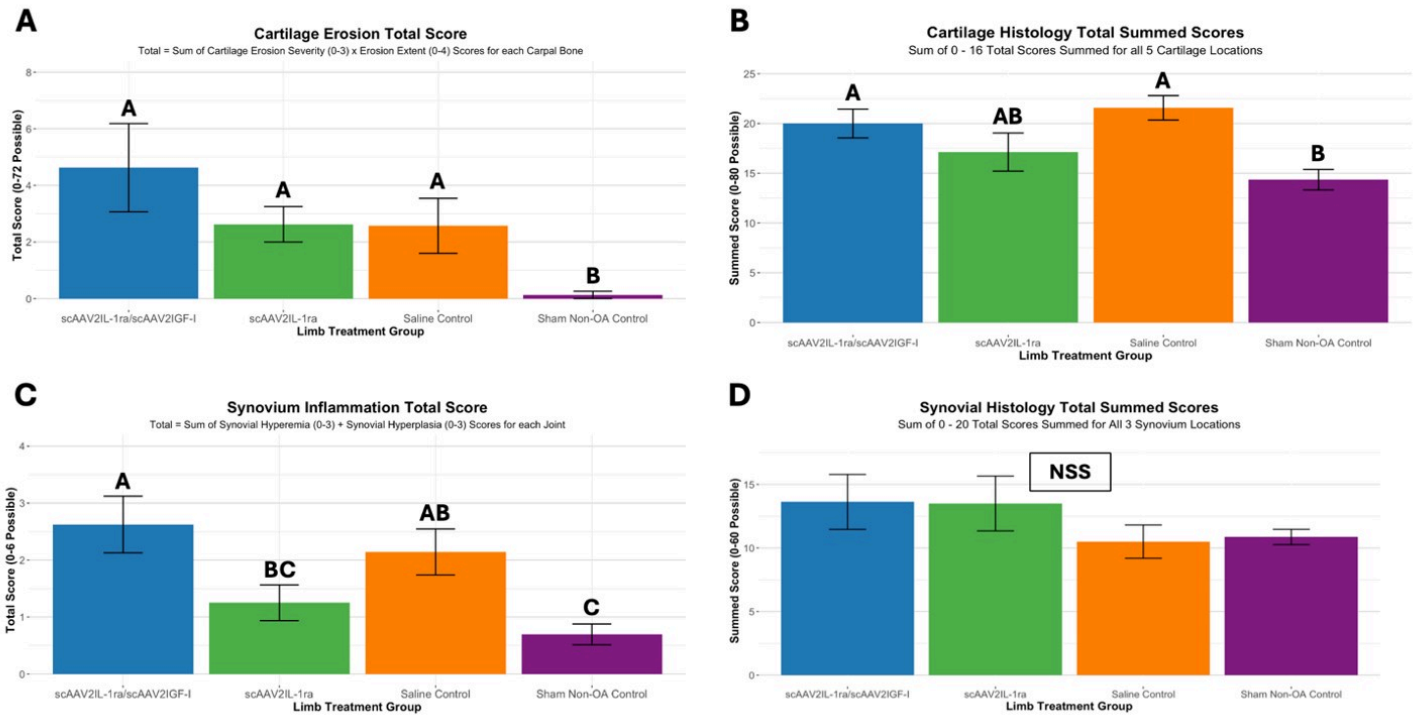


Figure 8

Effects of the scAAV2 treatments on macroscopic and microscopic indicators of OA pathology.

(A) The scAAV2IL-1ra/scAAV2IGF-I treated group had the highest cartilage (worst) erosion total score (most OA progression) from gross examination, while the scAAV2IL-1ra treated and saline control groups had similar, lower cartilage erosion total scores. All three treated groups had a statistically significant increase in cartilage erosion total score as compared to the non-OA sham control group (p-values listed in Supplementary Materials). **(B)** Total cartilage histological scores summed from the five carpal bones sampled (radial, 2^{nd}, 3^{rd}, 4^{th} and ulnar carpals). The scAAV2IL-1ra treated group showed the lowest mean summed scores (least OA progression) of the three treated groups and was the only treated group that did not show a statistically significant increase in total summed score as compared to the non-OA sham control group. **(C)** The scAAV2IL-1ra treated group had the lowest synovium inflammation total score (least OA progression) as graded via gross examination of the groups that received PTOA induction; displaying a statistically significant decrease in score as compared to the scAAV2IL-1ra/scAAV2IGF-I treated group (p-value=0.0296). Both the scAAV2IL-1ra/scAAV2IGF-I treated and saline control groups had a statistically significant increase in synovium inflammation total score as compared to the non-OA sham control group (p-values=0.0001 & 0.0046 respectively). **(D)** Total synovium histological scores summed from the three joint locations sampled (center, medial, and lateral). The saline control group had a slightly lower mean total summed score as compared to the other treated groups, although no statistically significant differences were found between any groups. All data displayed as mean +/- standard error.

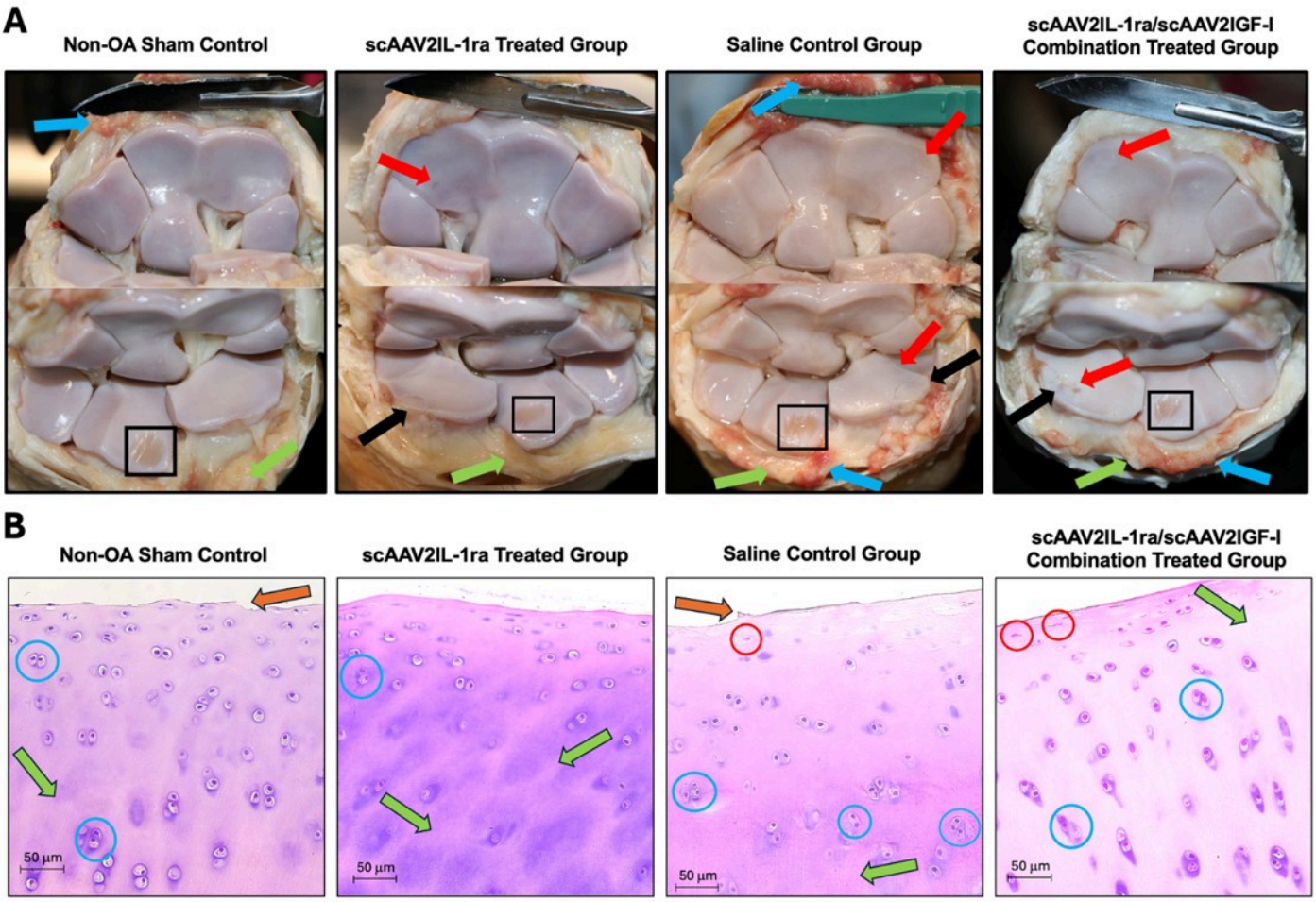


Figure 9

Representative gross images highlighting cartilage erosion and synovium inflammation (A) and representative 20x photomicrographs from 5mm sections of radial carpal cartilage sections stained with H&E (B). (A) Gross images highlighting the osteochondral chip fragment (black arrows) in the radial carpal (non-OA sham control joints did not receive chips), cartilage erosion (red arrows) and synovial inflammation for hyperemia and hyperplasia, denoted via blue and green arrows respectively. Black boxes indicate the site of cartilage samples harvested from the intermediate carpal for GAG synthesis assay before gross scoring (data not shown). Images are representative of cartilage erosion and synovium inflammation total scores. The non-OA sham joints displayed the fewest gross indicators of both cartilage erosion and synovium inflammation. The scAAV2IL-1ra and saline control joints typically displayed fewer gross indicators of cartilage erosion as compared to the scAAV2IL-1ra/scAAV2IGF-I treated joints. Additionally, the scAAV2IL-1ra treated joints typically showed the fewest gross indicators of synovium inflammation of all PTOA groups. **(B)** Images are representative of the total cartilage histology scores, which include fibrillation (orange arrows), chondrone formation (blue circles), chondrocyte necrosis (red circles), and focal cell loss (green arrows) at the radial carpal (site of chip fragment). Non-OA sham joints typically showed the fewest microscopic indicators of OA progression at the radial carpal. In terms of individual scoring metrics, the saline control group had slightly higher mean

scores for cartilage fibrillation, chondrocyte necrosis, and focal cell loss as compared to all other groups at the radial carpal. Additionally, it was the only treated group to show a statistically significant increase in chondrone formation (greater chondrone formation) as compared to the non-OA sham control (p-value=0.0172).

Supplementary Files

This is a list of supplementary files associated with this preprint. Click to download.

- MultiVectorTrialManuscriptAppendixA.docx
- MultiVectorTrialManuscriptSupplementalFigures.docx